

ARQ ANALYSIS UNDER FINITE-STATE HIDDEN MARKOV MODELS

APPROVED BY SUPERVISORY COMMITTEE:

---

Dr. Aria Nosratinia, Chair

---

Dr. Andrea Fumagalli

---

Dr. John Fonseca

Copyright 2005

Kamtorn Ausavapattanakun

All Rights Reserved

To my parents

ARQ ANALYSIS UNDER FINITE-STATE HIDDEN MARKOV MODELS

by

KAMTORN AUSAVAPATTANAKUN, B.E.

THESIS

Presented to the Faculty of  
The University of Texas at Dallas  
in Partial Fulfillment  
of the Requirements  
for the Degree of

MASTER OF SCIENCE IN ELECTRICAL ENGINEERING

THE UNIVERSITY OF TEXAS AT DALLAS

August 2005

## ACKNOWLEDGEMENTS

I would like to thank Dr. Aria Nosratinia for giving me an opportunity to do research as a graduate student with him. I express my gratitude to Dr. Nosratinia for his support, guidance and advice not only in my work but also in other aspects of my life. It is a wonderful experience to work with him.

I would like to thank Dr. Fumagalli and Dr. Fonseka for serving on my supervisory committee. I also thank my colleagues at the Multimedia Communications Laboratory for their help and support. They are a special group of people - intelligent, enthusiastic and humorous. Thanks especially to Shahab for being very helpful in the beginning of my research.

I would like to thank my family for their encouragement and support. I greatly thank my mother who inspired me to pursue Master degree and my father who gives me his full support for everything I do.

July 2005

# ARQ ANALYSIS UNDER FINITE-STATE HIDDEN MARKOV MODELS

Kamtorn Ausavapattanakun, M.S.E.E.

The University of Texas at Dallas, 2005

Supervisor: Dr. Aria Nosratinia

In this work, we analyze two basic ARQ protocols, Go-Back-N (GBN) and Selective Repeat (SR). Previous analyses of ARQ protocol have concentrated on simple two-state Markov models. We solve a wider class of problems by characterizing both the forward and reverse channels by finite-state hidden Markov models. We show that a Hidden Markov Model (HMM) can describe a block fading channel. We then calculate the throughput of GBN with reliable feedback, as well as unreliable feedback using block transition probabilities.

We also calculate the throughput and delay of SR ARQ under HMM. The moment generating function (MGF) technique is used to find throughput and delay. To calculate the MGF, we construct *matrix* signal flow graphs for the hidden Markov process. This procedure can be useful for a variety of other HMM problems and is therefore of interest by itself. Practical issues such as erasure errors and timeouts are included in our analyses, which are verified by extensive simulations.

## TABLE OF CONTENTS

Acknowledgements	v
Abstract	vi
List of Figures	ix
Chapter 1. Introduction	1
1.1 ARQ Protocols . . . . .	1
1.2 Wireless Fading Channel Models . . . . .	2
1.3 ARQ Analysis . . . . .	3
1.4 Scope and Outline of the Thesis . . . . .	4
Chapter 2. Analysis of Go-Back-N ARQ	6
2.1 Channel Models . . . . .	6
2.1.1 Hidden Markov Models . . . . .	6
2.1.2 Block Fading as a Hidden Markov Model . . . . .	8
2.1.3 Channels with Noisy Feedback . . . . .	10
2.2 Analysis in Reliable Feedback . . . . .	11
2.3 Analysis in Unreliable Feedback . . . . .	13
2.4 Numerical Results . . . . .	17
2.5 Summary . . . . .	20
Chapter 3. Analysis of Selective Repeat ARQ	21
3.1 Matrix Signal Flow Graphs . . . . .	21
3.2 Protocol Description . . . . .	25
3.3 Throughput Analysis . . . . .	26
3.4 Delay Analysis . . . . .	30
3.5 Numerical Results and Discussions . . . . .	32
3.6 Summary . . . . .	44

Chapter 4. Conclusion and Future Work	45
Bibliography	47
VITA	

## LIST OF FIGURES

2.1	A diagram of a hidden Markov channel where $S_t$ is the Markov channel state and $X_t$ is the Bernoulli observation . . . . .	7
2.2	A diagram of a block fading where the channel condition $Y_t$ changes only once every $N$ time intervals . . . . .	8
2.3	The state transition diagram of block fading with two channel qualities . . .	9
2.4	The state transition diagram of a finite state machine representing the transmitter of GBN protocol . . . . .	12
2.5	Throughput, $\eta$ , vs. $q$ : analytical and simulation results for $r = 0.3$ , $\varepsilon_G = 0.2$ , $\varepsilon_B = 0.8$ and $N = 1, 2, 3$ . . . . .	17
2.6	Throughput, $\eta$ , vs. Length of Block Fading, $N$ for $\varepsilon_G = 0.1$ , $\varepsilon_B = 0.7$ , Block error rate = 0.25 and $r = 0.1, 0.2, 0.3$ . . . . .	18
2.7	Throughput vs. block error rate in a Markov channel for $r = 0.3$ , $k = 5$ and $T = 5, 6, 7$ . . . . .	19
2.8	Throughput vs block error rate in block fading for $N = 3$ , $r = 0.3$ , $\varepsilon_G = 0.07$ , $\varepsilon_B = 0.7$ , $k = 5$ and $T = 5, 6, 7$ . . . . .	19
3.1	Three basic equivalences. (a) parallel, (b) series and (c) self-loop. . . . .	22
3.2	Matrix flow graph for throughput analysis of SR Protocol in reliable feedback	23
3.3	Matrix flow graph for throughput analysis of SR Protocol in unreliable feedback with $T = k$ . . . . .	26
3.4	Simplified matrix flow graph for throughput analysis of SR Protocol in unreliable feedback with $T = k$ . . . . .	26
3.5	Simplified matrix flow graph for throughput analysis of SR Protocol in unreliable feedback with $T > k$ . . . . .	28
3.6	The finite state machine to derive the probability vector of transmitting a new frame. . . . .	29
3.7	Matrix flow graph for delay analysis of SR Protocol in unreliable feedback	30
3.8	Throughput, $\eta$ and delay, $D$ , vs. block error rate, $\epsilon$ in Markov errors for $r = 0.3$ and $k = 5$ . . . . .	33
3.9	Throughput, $\eta$ and delay, $D$ , vs. block error rate, $\epsilon$ in Markov errors without NACK for $r = 0.3$ and $k = 5$ . . . . .	34
3.10	Throughput, $\eta$ and delay, $D$ , vs. block error rate, $\epsilon$ in hidden Markov errors for $r = 0.3$ , $\varepsilon_G = 0.07$ , $\varepsilon_B = 0.7$ and $k = 5$ . . . . .	36

3.11	Throughput, $\eta$ and delay, $D$ , vs. block error rate, $\epsilon$ in hidden Markov errors without NACK for $r = 0.3, \epsilon_G = 0.07, \epsilon_B = 0.7$ and $k = 5$ . . . . .	37
3.12	Throughput, $\eta$ and delay, $D$ , vs. block error rate, $\epsilon$ in block fading for $N = 3, r = 0.3, \epsilon_G = 0.07, \epsilon_B = 0.7$ and $k = 5$ . . . . .	38
3.13	Throughput, $\eta$ and delay, $D$ , vs. block error rate, $\epsilon$ in block fading with out NACK for $N = 3, r = 0.3, \epsilon_G = 0.07, \epsilon_B = 0.7$ and $k = 5$ . . . . .	39
3.14	Throughput, $\eta$ and delay, $D$ , vs. timeout, $T$ in Markov errors for $\epsilon = 0.3$ and $k = 5$ and in HMM for $\epsilon = 0.3, \epsilon_G = 0.07, \epsilon_B = 0.7$ and $k = 5$ . . . . .	40
3.15	Throughput, $\eta$ and delay, $D$ , vs. block error rate, $\epsilon$ in Markov errors for $r = 0.1$ and $k = 5$ . . . . .	41
3.16	Throughput, $\eta$ and delay, $D$ , vs. block error rate, $\epsilon$ in hidden Markov errors for $r = 0.1, \epsilon_G = 0.07, \epsilon_B = 0.7$ and $k = 5$ . . . . .	42
3.17	Throughput, $\eta$ and delay, $D$ , vs. block error rate, $\epsilon$ in block fading for $N = 3, r = 0.1, \epsilon_G = 0.07, \epsilon_B = 0.7$ and $k = 5$ . . . . .	43

## CHAPTER 1

### INTRODUCTION

#### 1.1 ARQ Protocols

Error control techniques are used to provide reliable communications over noisy channels. The commonly used techniques are Forward Error Correction (FEC), Automatic Repeat reQuest (ARQ) or a combination of them called hybrid-ARQ. In ARQ, data is protected by error detecting codes. If the receiver detects errors, the corresponding frame will be retransmitted.

There are three basic ARQ protocols namely Stop-and-Wait (SW), Go-Back-N (GBN) and Selective Repeat (SR). In SW, after sending a frame, the transmitter waits for feedback. A new frame is transmitted only when a positive acknowledgment (ACK) for the current frame is received. In contrast to SW, both GBN and SR protocols transmit frames continuously without waiting for acknowledgment messages. So GBN and SR are collectively called continuous ARQ protocols.

GBN is designed to operate without a re-ordering buffer at the receiver. Whenever a frame is missing or erroneous, the receiver simply discards all subsequent frames and sends no feedback for these discarded frames. So the transmitter has to retransmit all frames, starting with the erroneous one. If the error rate is high, the GBN protocol is inefficient.

In SR, only lost frames are retransmitted. Subsequent frames, which are correctly received, are stored in the receiver buffer so that the frames are sent to higher layer in the correct order. Because only lost frames are retransmitted, SR protocol is more efficient,

resulting in higher throughput. Therefore there is a trade-off between bandwidth and buffer space. Depending on the availability of these resources, GBN or SR protocol will be used.

## 1.2 Wireless Fading Channel Models

ARQ protocols have long been analyzed when channels are subject to independent errors and reliable feedback. However, this assumption is not valid for wireless channels subject to time-varying fading. To capture the temporal dynamics of wireless channel, a simple two-state Markov model is frequently used. However, the two-state Markov chain is not an accurate model for fading channels.

Kanel and Sastry [1] review different models (including Gilbert-Elliott model) for channels with memory. Wang and Chang [2] use mutual information to verify that a first-order Markov process can accurately model Rayleigh fading channel. The result is confirmed by a study in [3].

Markov models for wireless fading channels have been intensively investigated. In [4], the Rayleigh fading channel is modeled by finite-state Markov chain where a probability of error is associated with each state and Markov transitions between states are assumed. Received Signal-to-Noise Ratio (SNR) is partitioned into a finite number of intervals. Each interval is represented by a channel state. The probability of error for each state is calculated using the p.d.f. of the received SNR. Assuming slow fading, the transition probabilities are approximated by the ratio of the expected level crossing rate and the average symbols per second. Zhang and Kassam [5] develop and analyze a methodology to partition the received SNR.

Tan and Beaulieu [6] examine the validity of first-order Markov chains for Rayleigh fading channel. Instead of using mutual information, autocorrelation function (ACF) of

both processes are compared. Because Markov processes have an exponentially decaying ACF, the shape of the ACF is quite different from the fading channel's. A new method of modeling a fading channel is proposed in [7]. The Markov states are given by not only partitioning the amplitude of fading envelope but also the variation speed. The model is a better fit of the ACF of a fading process.

These models can be called Hidden Markov Models (HMM) because the transmission condition of a frame depends on the Markov states which are unobservable. Turin [8] demonstrate that fading channel can be accurately modeled by HMMs. Even through the two state Markov channels are traceable and simple to analyze, a number of states with arbitrary probabilities of error might be required to accurately model fading channels.

### 1.3 ARQ Analysis

Throughput of Go-Back-N (GBN) under two-state Markov and  $k$ -order Markov channels has been reported respectively in [9] and [10]. Both results assume error-free feedback. Several papers [11, 12, 13] have analyzed GBN protocol when both forward and reverse channels are described by two-state Markov errors. When the feedback is unreliable, a mechanism is required to prevent deadlock. Cho and Un [12] studied two GBN ARQ schemes, one with timer control and the other with buffer control. However, with timer control, their result is actually upper bound of the throughput. The result in [11] is a special case of the timer control in which the timer value equals round trip time. The throughput of GBN with any timer value is presented in [13]

Turin [14] calculates the throughput of GBN under hidden Markov model (HMM)<sup>1</sup>. The result is in the matrix form and can apply to any finite-state Markov channel but valid for channels with reliable feedback or bit-reversal feedback errors. Nonetheless, our

---

<sup>1</sup>The Markov model is, trivially, a special case of the HMM.

work has been influenced by the representation of a hidden Markov model in [14].

Throughput of Selective Repeat (SR) ARQ has been previously analyzed under certain conditions. In particular, it is known that when the average packet failure probability is  $\epsilon$ , the throughput of the Selective Repeat ARQ is  $1 - \epsilon$ . This simple answer is independent of channel dynamics, but is valid only when feedback is reliable [10]. When the feedback is unreliable, the analysis becomes complicated. Several works have studied the throughput of SR under two-state Markov channels with noisy feedback. The feedback errors are modeled either by independent errors [11] or by a simple two-state Markov process [12, 15, 16]. To date, the throughput of SR ARQ has not been analyzed under more elaborate channel models.

In SR ARQ, there are three components of delay time called queuing delay, transmission delay and re-sequencing delay. In this thesis, as we calculate the transmission delay of SR ARQ, we use delay as a shorthand for transmission delay. In reliable feedback, the transmission delay can be calculated from the throughput using Little's formula in queuing theory (assuming the transmitter always have a frame to send). Kim and Krunz [17] studied the total delay in a two-state Markov model. Defined as the sum of transmission and re-sequencing delay, delivery delay under Markov channels is derived in [18, 19]. Delay for in-sequence delivery of a higher-layer message consisting of multiple link-layer frames has been presented in [20].

#### 1.4 Scope and Outline of the Thesis

In this work, we analyze the performance of two basic ARQs, Go-Back-N (GBN) and Selective Repeat (SR) under very general conditions for both the forward and reverse channels. As discussed above, a wireless fading channel can be accurately described by a hidden Markov model (HMM). We show that block fading, a popular model for slow

fading channels [21], can also be characterized as a HMM. Under HMM, we extend existing results on throughput of GBN as well as present new results on throughput and delay of SR. We assume the source always has data to transmit. To prevent deadlock when a NACK is lost in transition, we use a time-out mechanism in both protocols.

We first generalize the results in [14] to find the throughput of GBN protocol. In unreliable feedback, Turin [14] assumed bit-reversal errors, thus an error in the feedback link would convert ACK to NACK and vice versa. Unfortunately this does not match common practice. Modern packet communication systems use CRC to detect any errors, and erroneous packets are discarded (erasure). We are able to address erasure errors on both the forward and reverse link by using block-transition probabilities.

In SR analysis, We use the moment generating function approach, and for calculation we employ the flow graph technique of Mason, which has been used for ARQ analysis in [22, 10, 12]. However, the flow graph methods in the existing literature cannot conveniently solve the multi-state Markov or the hidden Markov problem. We construct, for the hidden Markov processes, an extension of Mason graphs with matrix-valued link labels. Flow graphs with matrix labels, called matrix signal flow graphs (MSFG), were introduced in 1957 for the purpose of multi-terminal circuit analysis [23], but have not seen widespread use.

We use the MSFG to calculate the moment generating functions of two important random variables: transmission time (how many times a packet must be transmitted) and delay. From the generating functions, the average throughput and delay can be computed.

The outline of this thesis is as follows. Chapter 2 presents the analysis of GBN protocol. The channel models used in our analyses are also discussed in this chapter. The analysis of SR ARQ is presented in Chapter 3 including discussion of matrix flow graphs. There are numerical results which verify the correctness of our analysis in both chapters.

## CHAPTER 2

### ANALYSIS OF GO-BACK-N ARQ

In this chapter, we provide throughput analysis of GBN ARQ under Hidden Markov Models (HMM). We show that block fading can be represented by HMM. We then discuss the results in [14] which can calculate the throughput of GBN under HMM with reliable feedback. In noisy feedback, We assume erasure errors in the reverse channel and analyze the throughput of GBN ARQ. Simulations verify our analysis.

#### 2.1 Channel Models

##### 2.1.1 Hidden Markov Models

At time  $t$ , the status of each transmission, denoted by  $X_t$ , is a Bernoulli random variable taking values in  $\mathcal{X} = \{0, 1\}$ , where value 0 denotes an error-free frame, and 1 means the frame is erroneous. The probability of error, denoted with  $\varepsilon$ , is a function of channel condition. This channel condition is modeled by a multi-state Markov process  $S_t$ , with states  $\mathcal{S} = \{1, 2, \dots, K\}$  and probability transition matrix  $\mathbf{P}$ . Each state  $S_t = j$  gives rise to a different error probability  $\varepsilon_j$ . We denote the set of all such probabilities  $\boldsymbol{\varepsilon} = [\varepsilon_1, \varepsilon_2, \dots, \varepsilon_K]$ . The process  $X_t$ , which is driven by the Markov process  $S_t$ , is called a *hidden Markov* process and is characterized by the quartet  $\{\mathcal{S}, \mathcal{X}, \mathbf{P}, \boldsymbol{\varepsilon}\}$ .

For the purposes of future analysis, it is useful to define the joint probabilities of

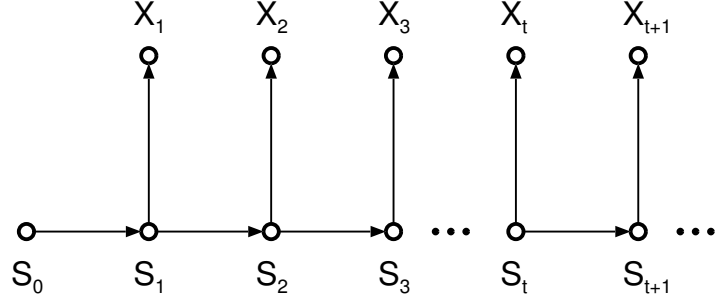


Figure 2.1. A diagram of a hidden Markov channel where  $S_t$  is the Markov channel state and  $X_t$  is the Bernoulli observation

channel state and observation at time  $t$ , given the channel state at time  $t - 1$

$$\begin{aligned}
 Pr(S_t = j, X_t = 1 | S_{t-1} = i) &= Pr(S_t = j | S_{t-1} = i) Pr(X_t = 1 | S_t = j, S_{t-1} = i) \\
 &= Pr(S_t = j | S_{t-1} = i) Pr(X_t = 1 | S_t = j) \\
 &= p_{ij} \varepsilon_j
 \end{aligned}$$

which we collect into a new matrix of transition probabilities  $\mathbf{P}_1 = \mathbf{P}\mathbf{B}_1$  where  $\mathbf{B}_1 = \text{diag}\{\varepsilon\}$ . Similarly

$$\begin{aligned}
 Pr(S_t = j, X_t = 0 | S_{t-1} = i) &= Pr(S_t = j | S_{t-1} = i) Pr(X_t = 0 | S_t = j, S_{t-1} = i) \\
 &= Pr(S_t = j | S_{t-1} = i) Pr(X_t = 0 | S_t = j) \\
 &= p_{ij}(1 - \varepsilon_j)
 \end{aligned}$$

which we collect into another matrix of transition probabilities  $\mathbf{P}_0 = \mathbf{P}\mathbf{B}_0$  where  $\mathbf{B}_0 = \text{diag}\{\mathbf{1} - \varepsilon\}$ . Figure 2.1 shows the transition of a hidden Markov channel.

Simply put,  $\mathbf{P}_0$  and  $\mathbf{P}_1$  are state transition probabilities when viewed jointly with (conditional) channel observations. Note that  $\mathbf{P}_0 + \mathbf{P}_1 = \mathbf{P}$ . With these definitions, it is possible to formulate the HMM with  $\{\mathcal{S}, \mathcal{X}, \mathbf{P}_0, \mathbf{P}_1\}$ . This equivalent formulation is similar to the one presented in [14] and is useful for the purposes of analysis. A similar construction is possible for larger observation alphabets, leading to more  $\mathbf{P}_i$  matrices.

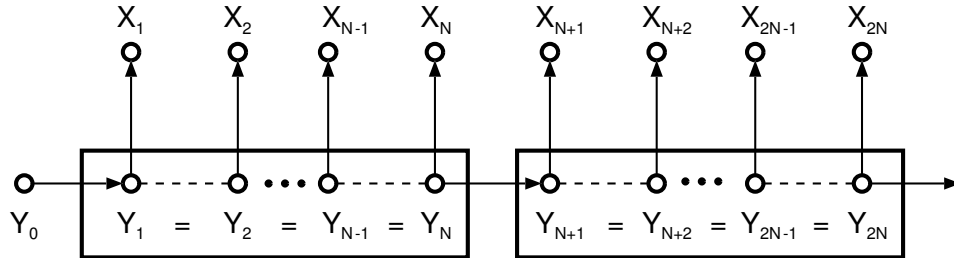


Figure 2.2. A diagram of a block fading where the channel condition  $Y_t$  changes only once every  $N$  time intervals

### 2.1.2 Block Fading as a Hidden Markov Model

The hidden Markov model can describe a number of physical channels, for example the fading wireless channel. However, for slow fading, often the *block fading* model is used, where the channel condition does not transition every time, but only once every  $N$  time intervals. Figure 2.2 shows the transition of a block fading channel. Thus, the transition probabilities of the channel are not time-invariant.

To cast the problem once again in the framework of hidden Markov processes, we need to expand the state space. We denote by  $Y_t$  the channel quality at time  $t$ , taking values from the set  $\mathcal{Y} = \{1, 2, \dots, K\}$ . Let the time index inside a block be represented by the index  $n$  taking values over  $\mathcal{N} = \{1, \dots, N\}$ . Then the expanded state space is defined as the Cartesian product  $s = (n, j)$  taking values over  $\mathcal{S} = \mathcal{N} \times \mathcal{Y}$ . The transition probabilities between the states are as follows. For  $i, j \in \mathcal{Y}$  and  $n = 1, 2, \dots, N - 1$

$$Pr[S_t = (m, i) | S_{t-1} = (n, j)] = \begin{cases} 1, & \text{if } m = n + 1 \text{ and } i = j \\ 0, & \text{otherwise} \end{cases} \quad (2.1)$$

For  $i, j \in \mathcal{Y}$  and  $n = N$

$$Pr[S_t = (m, i) | S_{t-1} = (n, j)] = \begin{cases} Pr[Y_t = i | Y_{t-1} = j], & \text{if } m = 1 \\ 0, & \text{otherwise} \end{cases} \quad (2.2)$$

Then  $S_t$  is a Markov chain whose state transition matrix we denote with  $\mathbf{M}$ . To write the state transition matrix, we need a linear ordering of the states. The ordering

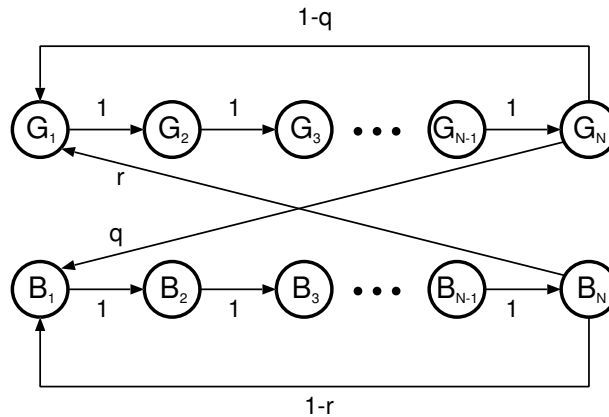


Figure 2.3. The state transition diagram of block fading with two channel qualities

does not affect the outcome of analysis, therefore we assume an arbitrary ordering and, with an abuse of notation, show it with the same symbol  $s = 1, 2, \dots, NK$ . In each state  $s$  the channel will have an error probability that we denote with  $\varepsilon_s$ , and the vector of all such probabilities is denoted with  $\boldsymbol{\varepsilon}$ .

For our examples we concentrate on the simple case where  $\mathcal{Y}$  has only two values, representing the good and bad fading situations. The state transition diagram is shown in Figure 2.3. For clarity the states are labeled  $\{G_1, B_1, \dots, G_N, B_N\}$ , where  $G_i$  and  $B_i$  represent the channel in a good or bad fading state, respectively, and the relative time index within fading block is  $i$ .

Thus we have arrived at a HMM described by the quartet  $\{\mathcal{S}, \mathcal{X}, \mathbf{M}, \boldsymbol{\varepsilon}\}$ , where  $\mathcal{S}$  is the state set,  $\mathcal{X} = \{0, 1\}$  is the observation set,  $\mathbf{M}$  is the state transition matrix and  $\boldsymbol{\varepsilon}$  is a vector of error probabilities in all (hidden) states. For the purposes of analysis, we follow the same formulation discussed above. Let  $\mathbf{A}_1 = \text{diag}\{\boldsymbol{\varepsilon}\}$  and  $\mathbf{A}_0 = \text{diag}\{\mathbf{1} - \boldsymbol{\varepsilon}\}$ . We have  $\mathbf{M}_0 = \mathbf{M}\mathbf{A}_0$  and  $\mathbf{M}_1 = \mathbf{M}\mathbf{A}_1$ . Then the HMM is fully specified with  $\{\mathcal{S}, \mathcal{X}, \mathbf{M}_0, \mathbf{M}_1\}$  [14].

### 2.1.3 Channels with Noisy Feedback

Now consider a channel with noisy feedback such that the forward and reverse channels are mutually independent and each is described by a hidden Markov model. Then the combined channel can also be characterized as a HMM, as shown below.

Let the forward and reverse channels respectively be  $\{\mathcal{S}^{(f)}, \mathcal{X}^{(f)}, \mathbf{P}_0^{(f)}, \mathbf{P}_1^{(f)}\}$  and  $\{\mathcal{S}^{(r)}, \mathcal{X}^{(r)}, \mathbf{P}_0^{(r)}, \mathbf{P}_1^{(r)}\}$ . The composite channel states are  $\mathcal{S}^{(c)} = \mathcal{S}^{(f)} \times \mathcal{S}^{(r)}$ , the Cartesian product of forward and reverse states. The transition probabilities of the composite states are

$$\begin{aligned} Pr(S_t^{(c)} = (j, m) | S_{t-1}^{(c)} = (i, k)) &= Pr(S_t^{(f)} = j, S_t^{(r)} = m | S_{t-1}^{(f)} = i, S_{t-1}^{(r)} = k) \\ &= Pr(S_t^{(f)} = j | S_{t-1}^{(f)} = i) Pr(S_t^{(r)} = m | S_{t-1}^{(r)} = k) \\ &= p_{ij}^{(f)} p_{km}^{(r)} \end{aligned}$$

Or, in compact notation,  $\mathbf{P}^{(c)} = \mathbf{P}^{(f)} \otimes \mathbf{P}^{(r)}$ , where  $\otimes$  denotes the Kronecker product of matrices. Note that the stationary vector of this transition matrix is  $\pi^{(c)} = \pi^{(f)} \otimes \pi^{(r)}$  where  $\pi^{(f)}$  and  $\pi^{(r)}$  are the stationary vectors of the transition matrices  $\mathbf{P}^{(f)}$  and  $\mathbf{P}^{(r)}$  respectively. We can also define the combined observation set to be  $\mathcal{X}^{(c)} = \mathcal{X}^{(f)} \times \mathcal{X}^{(r)} = \{00, 01, 10, 11\}$  where  $X_t^{(c)} = 00$  means both forward and reverse channels are good while  $X_t^{(c)} = 01$  means the reverse channel is erroneous. For  $X_t^{(c)} = 11$ , the joint probability of the combined observation and the composite state at time  $t$  given the composite state at time  $t - 1$  is

$$\begin{aligned} Pr(S_t^{(c)} = (j, m), X_t^{(c)} = 11 | S_{t-1}^{(c)} = (i, k)) \\ &= Pr(S_t^{(f)} = j, S_t^{(r)} = m, X_t^{(f)} = 1, X_t^{(r)} = 1 | S_{t-1}^{(f)} = i, S_{t-1}^{(r)} = k) \\ &= Pr(S_t^{(f)} = j, X_t^{(f)} = 1 | S_{t-1}^{(f)} = i) Pr(S_t^{(r)} = m, X_t^{(r)} = 1 | S_{t-1}^{(r)} = k) \\ &= (p_{ij}^{(f)} \varepsilon_j^{(f)}) \cdot (p_{km}^{(r)} \varepsilon_m^{(r)}) \end{aligned}$$

So we have  $\mathbf{P}_{11}^{(c)} = \mathbf{P}_1^{(f)} \otimes \mathbf{P}_1^{(r)}$ . The probability matrices for other observations can be found in the same way. Finally, the composite channel is characterized by  $\{\mathcal{S}^{(c)}, \mathcal{X}^{(c)}, \mathbf{P}_{00}^{(c)}, \mathbf{P}_{01}^{(c)}, \mathbf{P}_{10}^{(c)}, \mathbf{P}_{11}^{(c)}\}$  where  $\mathcal{S}^{(c)} = \mathcal{S}^{(f)} \times \mathcal{S}^{(r)}$ ,  $\mathcal{X}^{(c)} = \mathcal{X}^{(f)} \times \mathcal{X}^{(r)}$ , and each of the observation probability matrices is described by a Kronecker product, i.e.,  $\mathbf{P}_{ij}^{(c)} = \mathbf{P}_i^{(f)} \otimes \mathbf{P}_j^{(r)}$  for  $i, j = 0, 1$  (see also [24]).

## 2.2 Analysis in Reliable Feedback

Turin [14] calculate the throughput of GBN under this channel. The GBN transmitter is represented by a finite state machine with  $k + 1$  states where  $k$  is the round trip time. In state 0, an ACK is decoded and the next message is sent. In state 1, a NACK is decoded and the frame is retransmitted together with all subsequent frames. Then the transmitter has to wait for acknowledgment of the first frame. These waiting time is represented by states 2, 3,  $\dots$ ,  $k$ .

Let  $\mathbf{P}_{XA}$  and  $\mathbf{P}_{XN}$  be the probability matrix of decoding an ACK and NACK respectively and  $\mathbf{P}_{XX} = \mathbf{P}_{XA} + \mathbf{P}_{XN}$ . Also let  $\mathcal{Z} = \{0, 1, \dots, k\}$  represents these states. The state transition probabilities are as follows. For  $Z_{t-1} = 0$  and  $k$

$$Pr[Z_t = \ell | Z_{t-1}] = \begin{cases} \mathbf{P}_{XA}, & \text{if } \ell = 0 \\ \mathbf{P}_{XN}, & \text{if } \ell = 1 \\ \mathbf{0}, & \text{otherwise} \end{cases}$$

For  $Z_{t-1} = 1, 2, \dots, k - 1$

$$Pr[Z_t = \ell | Z_{t-1} = j] = \begin{cases} \mathbf{P}_{XX}, & \text{if } \ell = j + 1 \\ \mathbf{0}, & \text{otherwise} \end{cases}$$

Figure 2.4 show the state transition diagram of the GBN transmitter. Let  $\mathbf{T}$  be the block transition matrix and  $\hat{\pi} = [\pi_0 \ \pi_1 \ \dots \ \pi_k]$  be the stationary vector. Then the

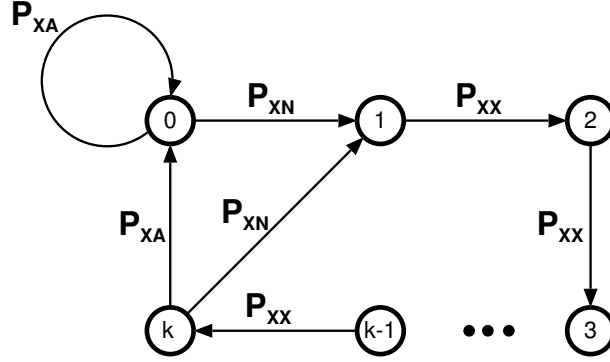


Figure 2.4. The state transition diagram of a finite state machine representing the transmitter of GBN protocol

stationary vector can be obtained by solving the following system of equations.

$$\begin{aligned}\hat{\pi}\mathbf{T} &= \hat{\pi} \\ \sum_{\ell \in \mathcal{Z}} \pi_{\ell} &= \pi\end{aligned}\quad (2.3)$$

where  $\pi$  is the stationary probabilities of the Markov state transition matrix. To find the throughput of GBN, we do not need to find all elements of the stationary vector. The throughput of GBN protocol is given by

$$\eta = \pi_0 \mathbf{1} = \pi [\mathbf{I} - \mathbf{P}_{XN} \mathbf{Q}(k)]^{-1} \mathbf{P}_{XA} \mathbf{1} \quad (2.4)$$

where  $\mathbf{I}$  is an identity matrix and  $\mathbf{Q}(k) = \sum_{i=0}^{k-2} \mathbf{P}_{XX}^i$ .

For example, consider block fading of length  $N = 3$  and two channel qualities (good and bad). Once every 3 time intervals, the channel quality is updated according to the transition matrix

$$\mathbf{P} = \begin{bmatrix} 1 - q & q \\ r & 1 - r \end{bmatrix} \quad (2.5)$$

where the first row and column corresponds to the good channel condition, and the second row and column to the bad channel condition. Now, for a Markov system that transitions *every time interval*, using Equation 2.1 and 2.2, the state transition probability matrix will be

$$\mathbf{M} = \begin{bmatrix} 0 & 0 & 1 & 0 & 0 & 0 \\ 0 & 0 & 0 & 1 & 0 & 0 \\ 0 & 0 & 0 & 0 & 1 & 0 \\ 0 & 0 & 0 & 0 & 0 & 1 \\ 1-q & q & 0 & 0 & 0 & 0 \\ r & 1-r & 0 & 0 & 0 & 0 \end{bmatrix} = \begin{bmatrix} \mathbf{0}_1 & \mathbf{I} \\ \mathbf{P} & \mathbf{0}_2 \end{bmatrix}$$

The error probability is equal to  $\varepsilon_G$  and  $\varepsilon_B$  for the states corresponding to the good and bad channel qualities, respectively. The vector of error probabilities is  $\boldsymbol{\varepsilon} = [\varepsilon_G \ \varepsilon_B \ \varepsilon_G \ \varepsilon_B \ \varepsilon_G \ \varepsilon_B]$ . The diagonal matrices of the state error and success probabilities are  $\mathbf{A}_1 = \text{diag}\{\boldsymbol{\varepsilon}\}$  and  $\mathbf{A}_0 = \mathbf{I} - \mathbf{A}_1$

Finally we have  $\{\mathcal{S}, \mathcal{X}, \mathbf{M}_0, \mathbf{M}_1\}$  as a HMM channel where  $\mathbf{M}_0 = \mathbf{M}\mathbf{A}_0$  and  $\mathbf{M}_1 = \mathbf{M}\mathbf{A}_1$ . Notice that the state transition probability  $\mathbf{M}$  is periodic with period  $N$  so the limiting state probabilities do not exist [25]. However, the stationary probabilities can be found by solving the following system of equations.

$$\begin{aligned} \pi\mathbf{M} &= \pi \\ \pi\mathbf{1} &= 1 \end{aligned} \tag{2.6}$$

where  $\mathbf{1}$  is a column vector of ones. Because the reverse channel is error-free, we have  $\mathbf{P}_{XA} = \mathbf{M}_0$ ,  $\mathbf{P}_{XN} = \mathbf{M}_1$  and  $\mathbf{P}_{XX} = \mathbf{M}_0 + \mathbf{M}_1 = \mathbf{M}$ . From Equation 2.4, the throughput of GBN protocol is

$$\eta = \pi[\mathbf{I} - \mathbf{M}_1\mathbf{Q}(k)]^{-1}\mathbf{M}_0\mathbf{1}$$

### 2.3 Analysis in Unreliable Feedback

Let the composite channel be characterized by  $\{\mathcal{S}, \mathcal{X}, \mathbf{M}_{00}, \mathbf{M}_{01}, \mathbf{M}_{10}, \mathbf{M}_{11}\}$ . In this context,  $X_t = 00$  means both channels are good while  $X_t = 01$  means the reverse channel is erroneous. Note that  $\mathbf{M} = \mathbf{M}_{00} + \mathbf{M}_{01} + \mathbf{M}_{10} + \mathbf{M}_{11}$ .

In [14], it is assumed that ACK errors are seen as NACK and vice versa, i.e., the transmitter will either decode ACK or NACK for every frame. Most data communication systems do not follow this model, however, as the frame in data link layer is normally protected by CRC. Thus we will assume feedback errors result in erasure. To prevent deadlock, we assume a timer mechanism is used as in [12]. Moreover, due to the nature of GBN, receiving ACK or NACK for the  $i$ th packet means all previous packets have been correctly received.

Both transmitter and receiver follow the rules of GBN protocol as in [13]. The timer is set when a frame is (re)transmitted. If the timer expires before any acknowledgments are received, the frame is retransmitted together with all the succeeding frames. So the timeout ( $T$ ) has to be greater than or equal to round trip time ( $T \geq k$ ). When ACKs or NACKs are erroneous, the transmitter will simply discard them. If the discarded frame is an ACK, the message can be implicitly acknowledged by subsequent ACKs or NACKs. If the discarded frame is a NACK, the transmitter has to wait until the timer expires.

Let us first consider the special case  $T = k$ . In this case when the acknowledgments are decoded incorrectly, the timer has expired and the message will be retransmitted immediately. Therefore the discarded ACK or NACK will have the same effect as NACK correctly received. So we have

$$\begin{aligned} \mathbf{P}_{XA} &= \mathbf{M}_{00} \\ \mathbf{P}_{XN} &= \mathbf{M}_{01} + \mathbf{M}_{10} + \mathbf{M}_{11} = \mathbf{M} - \mathbf{M}_{00} \end{aligned}$$

We can use Equation 2.4 to find the throughput in this scenario of  $T = k$ . Next consider the case  $T > k$ . Define  $d = T - k$  so that  $d$  is the maximum number of lost ACK before timer is expired. Then the transmitter can be represented by a finite state machine with  $T+d+1$  states, in state 0 an ACK is correctly decoded. States  $L_1, L_2, \dots, L_d$  correspond to 1, 2,  $\dots$ ,  $d$  lost ACKs respectively. Finally in states  $W_j, j = 1, 2, \dots, T$  the

transmitter is in the waiting period. Let  $\mathcal{Z} = \{0, L_1, L_2, \dots, L_d, W_T, W_{T-1}, \dots, W_1\}$  represent the set of all states. The block transition probabilities of these states can be given as follows.

For  $Z_{t-1} = 0, W_1$

$$Pr[Z_t = \ell | Z_{t-1}] = \begin{cases} \mathbf{M}_{00}, & \text{if } \ell = 0 \\ \mathbf{M}_{01}, & \text{if } \ell = L_1 \\ \mathbf{M}_{11}, & \text{if } \ell = W_T \\ \mathbf{M}_{10}, & \text{if } \ell = W_k \\ \mathbf{0}, & \text{otherwise} \end{cases} \quad (2.7)$$

For  $Z_{t-1} = L_1, L_2, \dots, L_{d-1}$

$$Pr[Z_t = \ell | Z_{t-1} = L_j] = \begin{cases} \mathbf{M}_{00}, & \text{if } \ell = 0 \\ \mathbf{M}_{01}, & \text{if } \ell = L_{j+1} \\ \mathbf{M}_{11}, & \text{if } \ell = W_{T-j} \\ \mathbf{M}_{10}, & \text{if } \ell = W_k \\ \mathbf{0}, & \text{otherwise} \end{cases} \quad (2.8)$$

For  $Z_{t-1} = L_d$

$$Pr[Z_t = \ell | Z_{t-1} = L_d] = \begin{cases} \mathbf{M}_{00}, & \text{if } \ell = 0 \\ \mathbf{M} - \mathbf{M}_{00}, & \text{if } \ell = W_k \\ \mathbf{0}, & \text{otherwise} \end{cases} \quad (2.9)$$

For  $Z_{t-1} = W_T, \dots, W_2$

$$Pr[Z_t = \ell | Z_{t-1} = W_j] = \begin{cases} \mathbf{M}, & \text{if } \ell = W_{j-1} \\ \mathbf{0}, & \text{otherwise} \end{cases} \quad (2.10)$$

Let  $\mathbf{T}$  be the block transition matrix and  $\hat{\pi} = [\pi_0 \ \pi_{L_1} \ \pi_{L_2} \ \dots \ \pi_{L_d} \ \pi_{W_T} \ \dots \ \pi_{W_1}]$  be the stationary vector. Then the stationary vector can be obtained by solving Equation 2.3 where  $\pi$  is the stationary probabilities of  $\mathbf{M}$  given in Equation 2.6. The throughput of GBN protocol is given by

$$\begin{aligned} \eta &= \{\pi_0 + (\pi_{L_1} + 2\pi_{L_2} + \dots + d\pi_{L_d}) (\mathbf{M}_{00} + \mathbf{M}_{10})\} \mathbf{1} \\ &= \left\{ \pi_0 + \left( \sum_{i=1}^d i\pi_{L_i} \right) (\mathbf{M}_{00} + \mathbf{M}_{10}) \right\} \mathbf{1} \end{aligned} \quad (2.11)$$

Let's consider an example of  $k = 5$  and  $T = 7$  as in [13]. So there are 10 states,  $\mathcal{Z} = \{0, L_1, L_2, W_7, \dots, W_1\}$  in the finite state machine. Denote the composite

channel with  $\{\mathcal{S}, \mathcal{X}, \mathbf{M}_{00}, \mathbf{M}_{01}, \mathbf{M}_{10}, \mathbf{M}_{11}\}$ . From Equations 2.7-2.10, the block transition probability matrix will be

$$\mathbf{T} = \begin{bmatrix} \mathbf{M}_{00} & \mathbf{M}_{01} & \mathbf{0} & \mathbf{M}_{11} & \mathbf{0} & \mathbf{M}_{10} & \cdots & \mathbf{0} \\ \mathbf{M}_{00} & \mathbf{0} & \mathbf{M}_{01} & \mathbf{0} & \mathbf{M}_{11} & \mathbf{M}_{10} & \cdots & \mathbf{0} \\ \mathbf{M}_{00} & \mathbf{0} & \mathbf{0} & \mathbf{0} & \mathbf{0} & \mathbf{M} - \mathbf{M}_{00} & \cdots & \mathbf{0} \\ \mathbf{0} & \mathbf{0} & \mathbf{0} & \mathbf{0} & \mathbf{M} & \mathbf{0} & \cdots & \mathbf{0} \\ \mathbf{0} & \mathbf{0} & \mathbf{0} & \mathbf{0} & \mathbf{0} & \mathbf{M} & \cdots & \mathbf{0} \\ & & & & & & \ddots & \\ \mathbf{0} & \mathbf{0} & \mathbf{0} & \mathbf{0} & \mathbf{0} & \mathbf{0} & \cdots & \mathbf{M} \\ \mathbf{M}_{00} & \mathbf{M}_{01} & \mathbf{0} & \mathbf{M}_{11} & \mathbf{0} & \mathbf{M}_{10} & \cdots & \mathbf{0} \end{bmatrix}$$

The stationary probability vectors are calculated from the following system of equations

$$\begin{aligned} \pi_0 &= (\pi_0 + \pi_{L_1} + \pi_{L_2} + \pi_{W_1})\mathbf{M}_{00} \\ \pi_{L_1} &= (\pi_0 + \pi_{W_1})\mathbf{M}_{01} \\ \pi_{L_2} &= \pi_{L_1}\mathbf{M}_{01} \\ \pi_{W_7} &= (\pi_0 + \pi_{W_1})\mathbf{M}_{11} \\ \pi_{W_6} &= \pi_{L_1}\mathbf{M}_{11} + \pi_{W_7}\mathbf{M} \\ \pi_{W_5} &= (\pi_0 + \pi_{L_1} + \pi_{W_1})\mathbf{M}_{10} + \pi_{L_2}(\mathbf{M} - \mathbf{M}_{00}) + \pi_{W_6}\mathbf{M} \\ \pi_{W_j} &= \pi_{W_{j+1}}\mathbf{M}, \quad j = 4, 3, 2 \text{ and } 1 \\ \sum_{\ell \in \mathcal{Z}} \pi_\ell &= \pi \end{aligned} \tag{2.12}$$

Substitute  $\mu = \pi_0 + \pi_{W_1}$ . After some algebra, the following equation is obtained which yields  $\mu$ .

$$\begin{aligned} \mu \{ &\mathbf{I} + \mathbf{M}_{01} + \mathbf{M}_{01}^2 + \mathbf{M}_{11} + \mathbf{M}_{01}\mathbf{M}_{11} + \mathbf{M}_{11}\mathbf{M} [\mathbf{M}_{10} + \mathbf{M}_{01}\mathbf{M}_{10} \\ &+ \mathbf{M}_{01}^2\mathbf{M} - \mathbf{M}_{01}^2\mathbf{M}_{00} + \mathbf{M}_{01}\mathbf{M}_{11}\mathbf{M} + \mathbf{M}_{11}\mathbf{M}\mathbf{M}] \mathbf{Q}(k) \} = \pi \end{aligned} \tag{2.13}$$

where  $\mathbf{I}$  is an identity matrix and  $\mathbf{Q}(k) = \sum_{i=0}^{k-2} \mathbf{M}^i$ . From the first three equations of

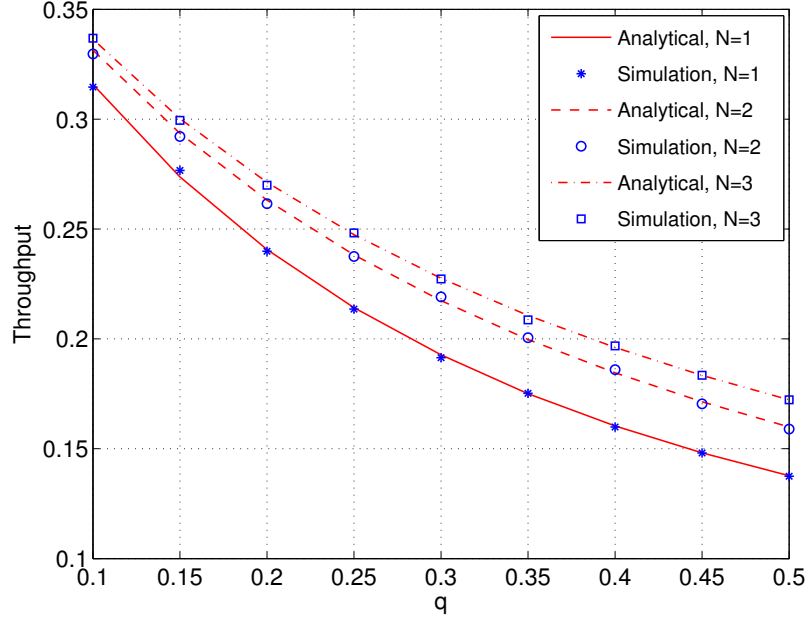


Figure 2.5. Throughput,  $\eta$ , vs.  $q$  : analytical and simulation results for  $r = 0.3$ ,  $\varepsilon_G = 0.2$ ,  $\varepsilon_B = 0.8$  and  $N = 1, 2, 3$

Equation 2.12, we have

$$\pi_0 = \mu(\mathbf{M}_{00} + \mathbf{M}_{01}\mathbf{M}_{00} + \mathbf{M}_{01}\mathbf{M}_{01}\mathbf{M}_{00})$$

$$\pi_{L_1} = \mu\mathbf{M}_{01}$$

$$\pi_{L_2} = \mu\mathbf{M}_{01}\mathbf{M}_{01}$$

Finally substituting  $\pi_0$ ,  $\pi_{L_1}$  and  $\pi_{L_2}$  into Equation 2.11 will give the throughput of GBN protocol.

## 2.4 Numerical Results

We compute numerical results for a channel with two quality levels, whose transition matrix is given in Equation 2.5. When feedback is reliable, the parameters of the forward channel are the probability of error in each state ( $\varepsilon_G$  and  $\varepsilon_B$ ), round trip time ( $k$ ), length of block fading ( $N$ ) and state transition probabilities ( $r$  and  $q$ ). The block

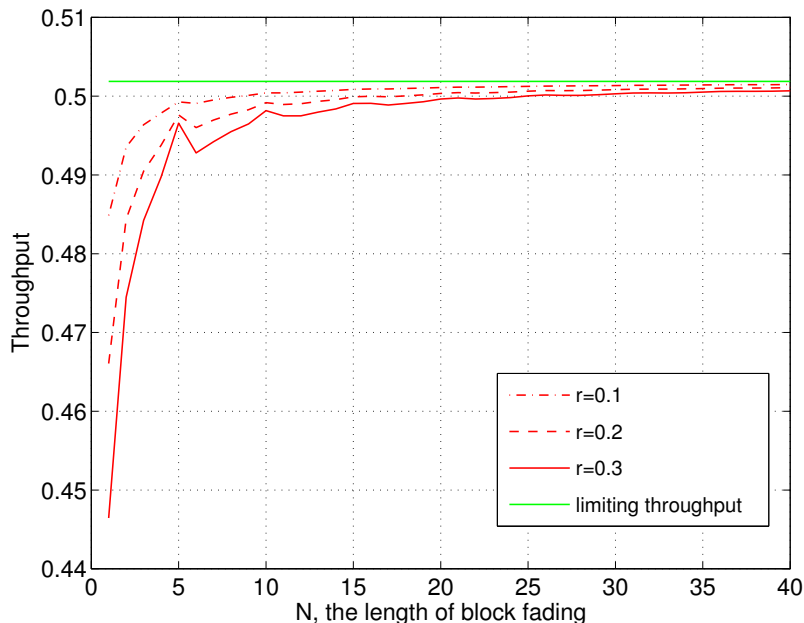


Figure 2.6. Throughput,  $\eta$ , vs. Length of Block Fading,  $N$  for  $\varepsilon_G = 0.1$ ,  $\varepsilon_B = 0.7$ , Block error rate = 0.25 and  $r = 0.1, 0.2, 0.3$

error rate will be sometimes used instead of  $q$ . The round trip time is set to 5 ( $k = 5$ ). Figure 2.5 shows the throughput vs  $q$  under block fading channel for  $N = 1, 2$ , and 3. The throughput under block fading channels is higher than i.i.d. channels when  $r + q < 1$  as reported in [9]. Figure 2.6 shows the throughput vs the length of block fading ( $N$ ), exhibiting a limiting throughput as  $N$  goes to infinity. Let  $\pi_G$  and  $\pi_B$  denote the good and bad steady state probabilities respectively and  $\eta_{iid}(P_e)$  denote the throughput of GBN protocol under i.i.d. channels with probability of error  $P_e$ . Then we have

$$\lim_{N \rightarrow \infty} \eta = \pi_G \eta_{iid}(\varepsilon_G) + \pi_B \eta_{iid}(\varepsilon_B)$$

This limit is shown in Figure 2.6. For the unreliable feedback case, we assume the reverse channel has the same statistics as the forward channel, i.e.,  $\{\mathcal{S}^{(f)}, \mathcal{X}^{(f)}, \mathbf{M}_1^{(f)}, \mathbf{M}_0^{(f)}\} = \{\mathcal{S}^{(r)}, \mathcal{X}^{(r)}, \mathbf{M}_0^{(r)}, \mathbf{M}_1^{(r)}\}$ . Because first-order Markov models are a special case of HMM, we first compare our results with the analytical results reported by [13] (Figure 2.7),

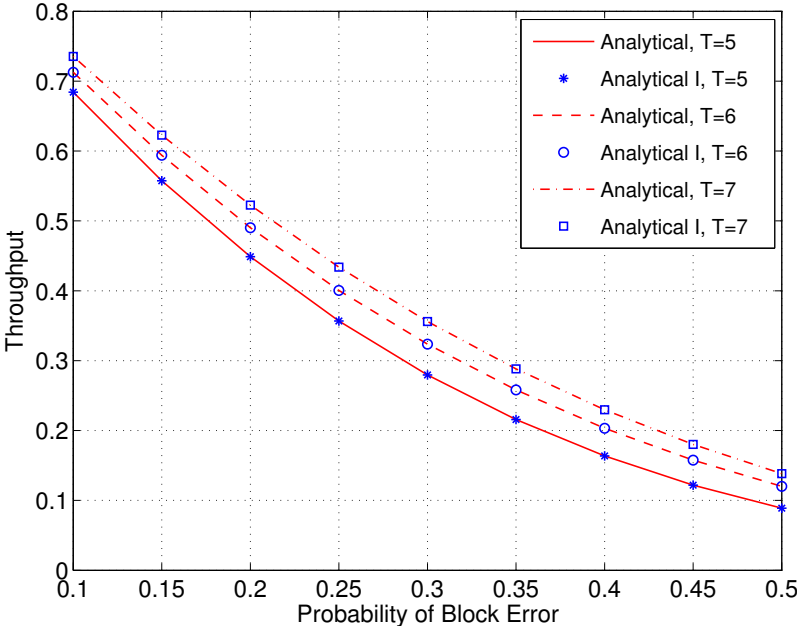


Figure 2.7. Throughput vs. block error rate in a Markov channel for  $r = 0.3$ ,  $k = 5$  and  $T = 5, 6, 7$

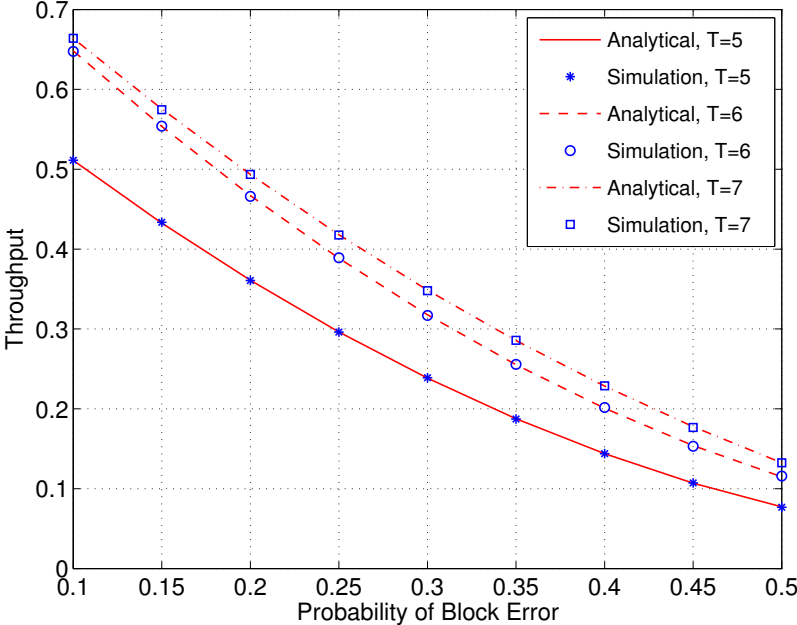


Figure 2.8. Throughput vs block error rate in block fading for  $N = 3$ ,  $r = 0.3$ ,  $\varepsilon_G = 0.07$ ,  $\varepsilon_B = 0.7$ ,  $k = 5$  and  $T = 5, 6, 7$

observing that the same throughput can be obtained by both methods. Then we plot the throughput under block fading channel with  $N = 3$  in Figure 2.8. The difference between the simulation and analytical result is negligible. Each of the above simulations uses at least 1 million frames. The 95% confidence interval for all simulations lies within  $\pm 0.2\%$  of the reported results.

## 2.5 Summary

We study Go-Back-N ARQ under hidden Markov channels. We show that Turin's results can apply to block fading which is generally neither Markov or hidden Markov channels. When feedback is unreliable, we assume erasure errors and calculate the throughput of GBN.

## CHAPTER 3

### ANALYSIS OF SELECTIVE REPEAT ARQ

We first give a brief overview of matrix signal graphs (MSFG), a new technique for analysis of ARQ protocols. From protocol description, we use MSFG to calculate the throughput and delay of SR ARQ. Our analysis is verified by simulation results.

#### 3.1 Matrix Signal Flow Graphs

A signal flow graph [26] is a diagram of directed branches connecting a set of nodes. The graph also represents a system of equations. The nodes are variables in the equations and the branch labels, a.k.a. branch transmissions, represent relationships among the variables. To simplify the flow graphs, there are three basic equivalences known as parallel, series and self-loop. These equivalences are shown in Figure 3.1. A thorough discussion of signal flow graphs can be found in [25].

Scalar flow graphs have been used to find the moment generating functions (MGF) of transmission time and delay time in throughput and delay analysis respectively [22, 10, 12]. The transmission time ( $\tau$ ) is defined as the number of frames being transmitted per a successful frame while the delay time ( $D$ ) is defined as the time from a frame is first transmitted to its ACK is received. Both transmission time and delay time are discrete random variables with positive integer outcomes. Using the MGF, the expected values can be calculated and the throughput is the reciprocal of the transmission time.

We briefly review the basic technique for building flow graphs. The graph nodes correspond to states of the transmitter. One input node (I) represents the start of trans-

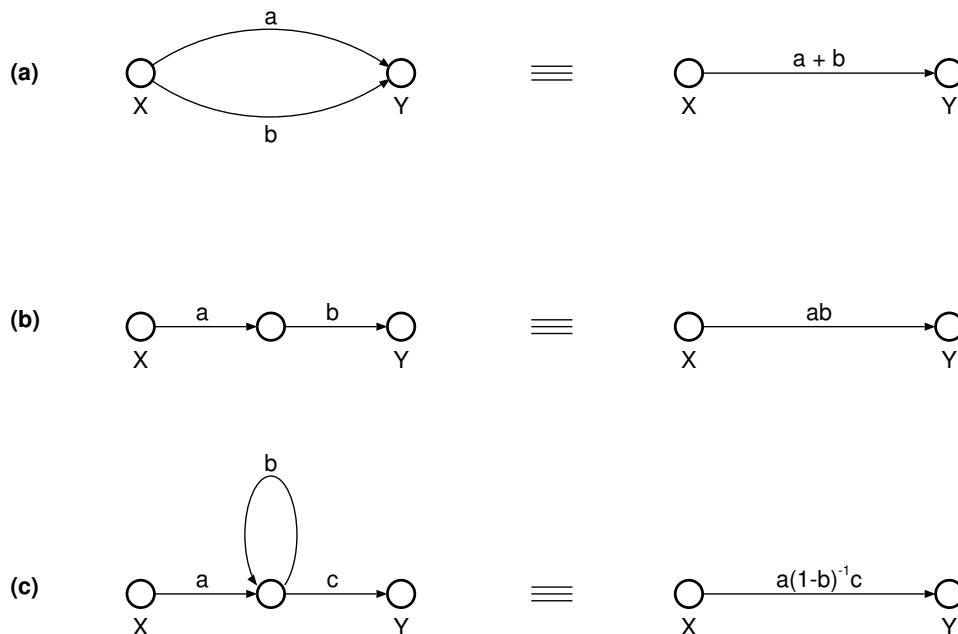


Figure 3.1. Three basic equivalences. (a) parallel, (b) series and (c) self-loop.

mission, and one output node (O) represents correct reception of acknowledgment. Other nodes represent intermediate states. As events in the network unfold, the transmitter goes from one state to the other. Each state transition takes a certain amount of time  $n$ , and a probability  $p$ , which together appear in the branch gain  $p z^n$ . The input-output gain of the entire graph is thus a polynomial in  $z$  whose coefficients are the probabilities of corresponding delay values. A moment's thought reveals that this is nothing but  $E[z^n]$ , the moment generating function.

Scalar flow graphs are useful for two-state Markov channels, but for multi-state models and hidden Markov models the flow graphs become prohibitively complicated. To streamline the analysis, we propose to label the branches with observation probability matrices. Flow graphs with matrix branch transmissions and vector node values are called matrix signal flow graphs (MSFG). In this method, the matrix gain of the graph is calculated using the usual basic operations, then the desired MGF is calculated by pre- and post-multiplications of row and column vectors respectively, as shown in the sequel.

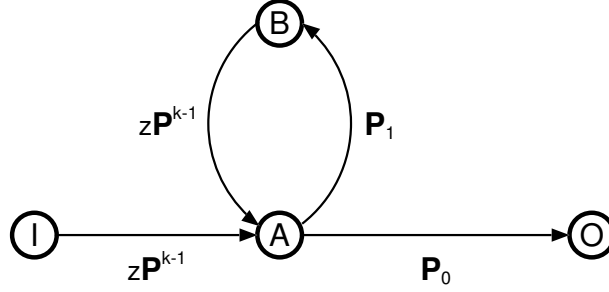


Figure 3.2. Matrix flow graph for throughput analysis of SR Protocol in reliable feedback

To demonstrate the MSFG methodology, we compute the throughput of SR ARQ in HMM with noiseless feedback. Let  $\mathbf{P}_0$  and  $\mathbf{P}_1$  respectively be the success and error probability matrices of a HMM.  $\mathbf{P} = \mathbf{P}_0 + \mathbf{P}_1$  is the state transition probability matrix. Let  $k$  be round trip time so that a feedback will be received  $k - 1$  time slots after a frame is sent.

Figure 3.2 shows the matrix flow graph for SR ARQ, assuming error-free feedback. In this figure, node I represents transmission of a new frame. Node A represents reception of a feedback. The feedback can either be an ACK (transition to node O) or a NACK (transition to node B). At node O, an ACK is received and the frame will exit the system. At node B, the lost frame will be retransmitted, so the loop between node A and B represents retransmission of the erroneous frame until it is correctly received. Using basic node reduction, the matrix generating function of transmission time will be

$$\begin{aligned}\Phi_\tau(z) &= z\mathbf{P}^{k-1} (\mathbf{I} - z\mathbf{P}_1\mathbf{P}^{k-1})^{-1} \mathbf{P}_0 \\ &= z (\mathbf{I} - z\mathbf{P}^{k-1}\mathbf{P}_1)^{-1} \mathbf{P}^{k-1}\mathbf{P}_0\end{aligned}$$

where  $\mathbf{I}$  is identity matrix. Let  $\pi_I$  be the probability vector of transmitting a new frame. In this simple case,  $\pi_I = \pi\mathbf{P}_0$  where  $\pi$  is the stationary vector of  $\mathbf{P}$ . The stationary vector

( $\pi$ ) can be found by solving the following system of equations

$$\begin{aligned}\pi\mathbf{P} &= \pi \\ \pi\mathbf{1} &= 1\end{aligned}\tag{3.1}$$

where  $\mathbf{1}$  is a column vector of ones. Let  $\epsilon$  be the frame error rate. In this scenario, we have  $\epsilon = \pi\mathbf{P}_1\mathbf{1}$  and  $1 - \epsilon = \pi\mathbf{P}_0\mathbf{1}$ . The generating function can be calculated by left- and right-multiplying the matrix generating function with the input row vector and the column vector of ones.

$$\begin{aligned}\phi_\tau(z) &= \frac{\pi_I\Phi_\tau(z)\mathbf{1}}{\pi_I\mathbf{1}} \\ &= \frac{1}{1-\epsilon}\pi\mathbf{P}_0\Phi_\tau(z)\mathbf{1}\end{aligned}\tag{3.2}$$

The average transmission time ( $\bar{\tau}$ ) can be found by evaluating the derivative of  $\phi_\tau(z)$  at  $z = 1$ . Substituting and taking the derivative, we get:

$$\begin{aligned}\bar{\tau} &= \frac{1}{1-\epsilon}\pi\mathbf{P}_0 \left[ (\mathbf{I} - \mathbf{P}^{k-1}\mathbf{P}_1)^{-1} \right. \\ &\quad \left. + (\mathbf{I} - \mathbf{P}^{k-1}\mathbf{P}_1)^{-1} \mathbf{P}^{k-1}\mathbf{P}_1 (\mathbf{I} - \mathbf{P}^{k-1}\mathbf{P}_1)^{-1} \right] \mathbf{P}^{k-1}\mathbf{P}_0\mathbf{1} \\ &= \frac{1}{1-\epsilon}\pi\mathbf{P}_0 (\mathbf{I} - \mathbf{P}^{k-1}\mathbf{P}_1)^{-1} (\mathbf{I} - \mathbf{P}^{k-1}\mathbf{P}_1)^{-1} \mathbf{P}^{k-1}\mathbf{P}_0\mathbf{1} \\ &= \frac{1}{1-\epsilon}\pi\mathbf{P}^{k-1}\mathbf{P}_0 (\mathbf{I} - \mathbf{P}^{k-1}\mathbf{P}_1)^{-1} (\mathbf{I} - \mathbf{P}^{k-1}\mathbf{P}_1)^{-1} \mathbf{P}^{k-1}\mathbf{P}_0\mathbf{1} \\ &= \frac{1}{1-\epsilon}\end{aligned}$$

where we have used the following identity for square matrices  $A$

$$\frac{d}{dz}(\mathbf{I} - \mathbf{A}z)^{-1} = (\mathbf{I} - \mathbf{A}z)^{-1} \mathbf{A} (\mathbf{I} - \mathbf{A}z)^{-1}$$

Throughput is the reciprocal of the average transmission time, thus  $\eta = 1/\bar{\tau} = 1 - \epsilon$ . The throughput of SR ARQ under HMM is therefore similar to the well-known previous results in  $k$ -order Markov channels [10].

### 3.2 Protocol Description

SR ARQ allows the receiver to accept frames out of order. The out-of-order frames will be stored in a buffer, sorted, and passed to higher layers in the correct order. For the purposes of this analysis we disregard buffer overflows. The feedback consists of ACKs and NACKs for error-free frames and erroneous frames respectively. The round trip time is  $k$ , i.e., it takes  $k - 1$  time slots between transmission of a frame and receipt of its feedback (ACK or NACK).

At the transmitter, a timeout mechanism is used to prevent deadlock. When a frame is (re)transmitted, the timeout associated with this frame is set to  $T$ . If the timeout expires and no acknowledgment is received, the frame will be retransmitted. Clearly the timeout has to be greater than or equal to the round trip time ( $T \geq k$ ).

We assume ACK/NACK will include the information about all correctly received frames. So the frame whose ACK is lost will be acknowledged by subsequent ACKs/NACKs. If the succeeding ACKs/NACKs is successfully received before timer expiration, the frame will not be retransmitted. When a frame is lost and its NACK is received, the frame will be retransmitted immediately. If the NACK is also lost, the frame will be retransmitted after timer expires.

In practice, ACK and NACK do not update the transmitter about the status of any previous frames. A frame whose ACK is lost has to always be retransmitted. We observe that the timeout has negligible effect on the throughput but it increases the delay, so to minimize the delay the timeout should be as small as possible ( $T = k$ ). The performance of SR variations are compared in Section 3.5.

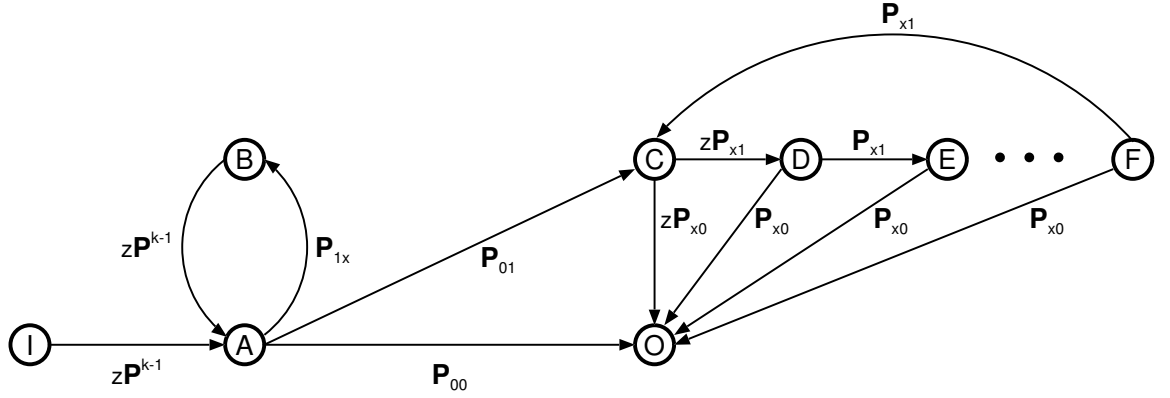


Figure 3.3. Matrix flow graph for throughput analysis of SR Protocol in unreliable feedback with  $T = k$

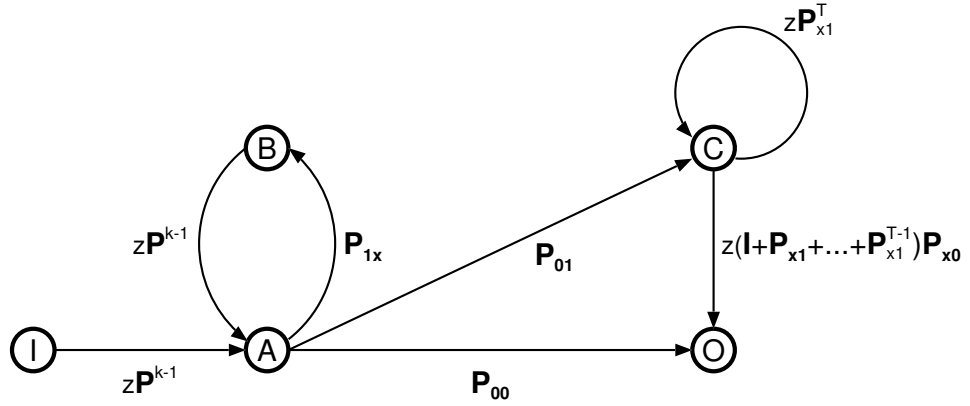


Figure 3.4. Simplified matrix flow graph for throughput analysis of SR Protocol in unreliable feedback with  $T = k$

### 3.3 Throughput Analysis

Consider the composite channel  $\{\mathcal{S}, \mathcal{X}, \mathbf{P}_{00}, \mathbf{P}_{01}, \mathbf{P}_{10}, \mathbf{P}_{11}\}$ . For simplicity, We define

$$\mathbf{P}_{0x} = \mathbf{P}_{00} + \mathbf{P}_{01}$$

$$\mathbf{P}_{1x} = \mathbf{P}_{10} + \mathbf{P}_{11}$$

$$\mathbf{P}_{x0} = \mathbf{P}_{00} + \mathbf{P}_{10}$$

$$\mathbf{P}_{x1} = \mathbf{P}_{01} + \mathbf{P}_{11}$$

So  $\mathbf{P}_{1x}$  is the probability matrix of error in the forward channel and  $\mathbf{P}_{x0}$  is the probability matrix of success in the reverse channel.

The flow graph in Figure 3.3 describes the operation of Selective Repeat ARQ, where the timeout equals the round trip time ( $T = k$ ). Node I represents that a new frame is transmitted. After sending the new frame, its feedback will be received  $k - 1$  time slots later. This state is represented by node A.

At this point there are three possibilities, an error-free ACK (transition to node O), an erroneous ACK (transition to node C) and an error-free or erroneous NACK (transition to node B).<sup>1</sup>

If ACK is correctly received, the frame will be removed from the system at node O. At node B, the lost frame will be retransmitted so that the loop between node A and B represents retransmission of the erroneous frame until it is correctly received. At node C, the ACK is lost and the timer expires so the frame will be retransmitted and the timeout will be reset. The frame will then be acknowledged when a succeeding ACK/NACK is correctly received. Nodes D, E and F represent the case where the subsequent ACK/NACK is erroneous. If the timer expires before receiving any ACKs/NACKs, the frame will be retransmitted again. This algorithm is expressed by the loop C-D-E-F. Using basic node reduction, the graph can be simplified as shown in Figure 3.4. For  $T = k$ , the matrix generating function (the input-output relationship) is

$$\Phi_{\tau}(z) = z\mathbf{P}^{k-1} (\mathbf{I} - z\mathbf{P}_{1x}\mathbf{P}^{k-1})^{-1} \left[ \mathbf{P}_{00} + \mathbf{P}_{01} (\mathbf{I} - z\mathbf{P}_{x1}^T)^{-1} z \left( \sum_{i=0}^{T-1} \mathbf{P}_{x1}^i \right) \mathbf{P}_{x0} \right]$$

We now generalize the timeout to an arbitrary value  $T > k$ . Let  $d = T - k$ . The matrix flow graph for this case is shown in Figure 3.5, and the matrix generating function is

---

<sup>1</sup>With timeout set to  $T = k$ , receiving an error-free NACK or an erroneous NACK has the same effect upon the transmitter. If NACK is received, frame is retransmitted. If it is lost, timeout expires and the frame is again retransmitted.

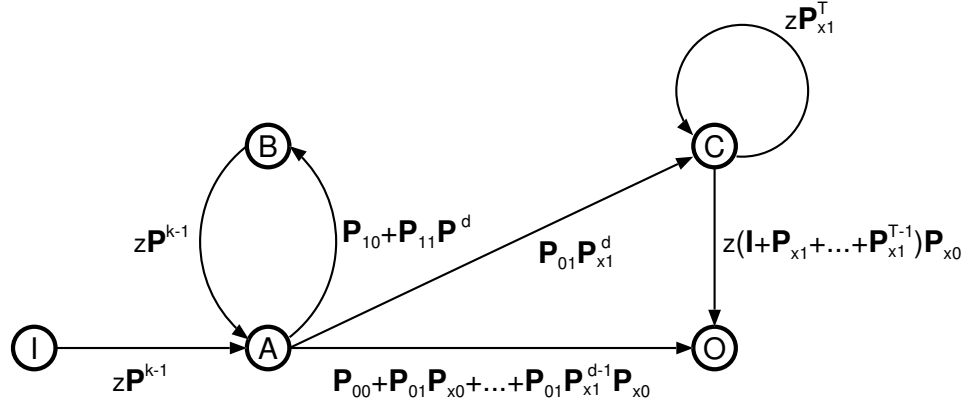


Figure 3.5. Simplified matrix flow graph for throughput analysis of SR Protocol in unreliable feedback with  $T > k$

$$\begin{aligned} \Phi_{\tau}(z) = & z\mathbf{P}^{k-1} (\mathbf{I} - z\mathbf{P}_{10}\mathbf{P}^{k-1} - z\mathbf{P}_{11}\mathbf{P}^{T-1})^{-1} \left[ \mathbf{P}_{00} + \mathbf{P}_{01} \left( \sum_{j=0}^{d-1} \mathbf{P}_{x1}^j \right) \mathbf{P}_{x0} \right. \\ & \left. + \mathbf{P}_{01}\mathbf{P}_{x1}^d (\mathbf{I} - z\mathbf{P}_{x1}^T)^{-1} z \left( \sum_{i=0}^{T-1} \mathbf{P}_{x1}^i \right) \mathbf{P}_{x0} \right] \end{aligned}$$

As mentioned earlier, to calculate the desired MGF, one also needs a vector probability, in this case  $\pi_I$ , the probability vector of transmitting a new frame. This is achieved by solving a system of equations involving several vector probabilities, which are derived as follows.

From Figures 3.4 and 3.5, node I, B, and C represent respectively transmission of a new frame, retransmission of an erroneous frame and retransmission of a frame that was correctly received, but its timer expires. We can simplify the graph with  $z = 1$  to consist of only these nodes as shown in Figure 3.6. Let  $\pi_I, \pi_B$  and  $\pi_C$  be the probability vectors of states I, B, and C, respectively. These probability vectors can be found by solving the

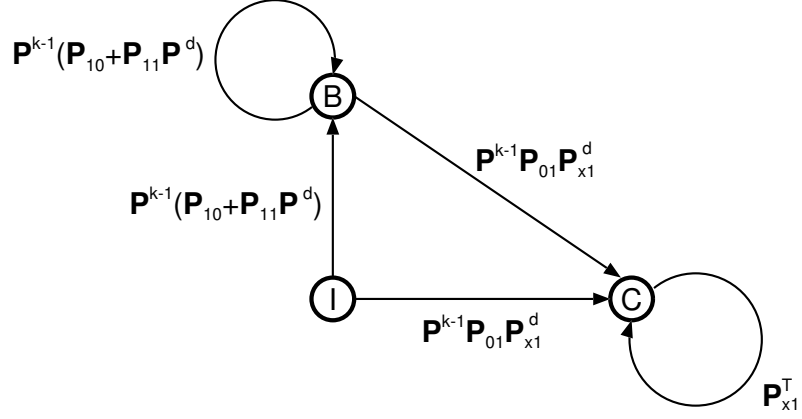


Figure 3.6. The finite state machine to derive the probability vector of transmitting a new frame.

following system of equations

$$\begin{aligned}
 \pi_B &= (\pi_I + \pi_B) \mathbf{P}^{k-1} (\mathbf{P}_{10} + \mathbf{P}_{11} \mathbf{P}^{T-k}) \\
 \pi_C &= (\pi_I + \pi_B) \mathbf{P}^{k-1} \mathbf{P}_{01} \mathbf{P}_{x1}^{T-k} + \pi_C \mathbf{P}_{x1}^T \\
 \pi &= \pi_I + \pi_B + \pi_C
 \end{aligned} \tag{3.3}$$

where the last equation comes from the fact that the transmitter always has a frame to transmit and  $\pi$  is the stationary vector of the state transition matrix. Solving for  $\pi_I$  from the system of equations 3.3, the generating function of transmission time ( $\phi_\tau$ ) can be derived by Equation 3.2. Substituting and taking the derivative, the expected transmission time is computed as follows. For  $T = k$ ,

$$\begin{aligned}
 \bar{\tau} &= \frac{1}{\pi_I \mathbf{1}} \pi_I \mathbf{P}^{k-1} \left\{ (\mathbf{I} - \mathbf{P}_{1x} \mathbf{P}^{k-1})^{-1} \mathbf{P}_{1x} \mathbf{P}^{k-1} (\mathbf{I} - \mathbf{P}_{1x} \mathbf{P}^{k-1})^{-1} \right. \\
 &\quad \cdot \left[ \mathbf{P}_{00} + \mathbf{P}_{01} (\mathbf{I} - \mathbf{P}_{x1}^T)^{-1} \left( \sum_{i=0}^{T-1} \mathbf{P}_{x1}^i \right) \mathbf{P}_{x0} \right] + (\mathbf{I} - \mathbf{P}_{1x} \mathbf{P}^{k-1})^{-1} \\
 &\quad \cdot \left[ \mathbf{P}_{00} + \mathbf{P}_{01} (\mathbf{I} - \mathbf{P}_{x1}^T)^{-1} \mathbf{P}_{x1}^T (\mathbf{I} - \mathbf{P}_{x1}^T)^{-1} \left( \sum_{i=0}^{T-1} \mathbf{P}_{x1}^i \right) \mathbf{P}_{x0} \right. \\
 &\quad \left. \left. + 2\mathbf{P}_{01} (\mathbf{I} - \mathbf{P}_{x1}^T)^{-1} \left( \sum_{i=0}^{T-1} \mathbf{P}_{x1}^i \right) \mathbf{P}_{x0} \right] \right\} \mathbf{1}
 \end{aligned}$$

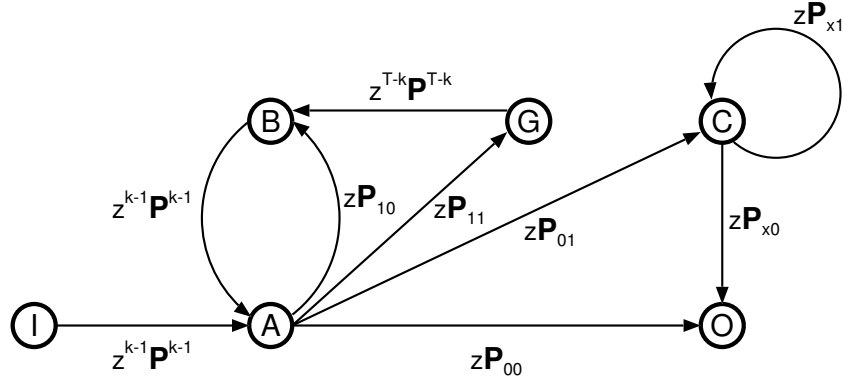


Figure 3.7. Matrix flow graph for delay analysis of SR Protocol in unreliable feedback

For  $T > k$ ,

$$\begin{aligned}
\bar{\tau} = & \frac{1}{\pi_I \mathbf{1}} \pi_I \mathbf{P}^{k-1} \left\{ (\mathbf{I} - \mathbf{P}_{10} \mathbf{P}^{k-1} - \mathbf{P}_{11} \mathbf{P}^{T-1})^{-1} (\mathbf{P}_{10} \mathbf{P}^{k-1} + \mathbf{P}_{11} \mathbf{P}^{T-1}) \right. \\
& \cdot (\mathbf{I} - \mathbf{P}_{10} \mathbf{P}^{k-1} - \mathbf{P}_{11} \mathbf{P}^{T-1})^{-1} \left[ \mathbf{P}_{00} + \mathbf{P}_{01} \left( \sum_{j=0}^{d-1} \mathbf{P}_{x1}^j \right) \mathbf{P}_{x0} + \mathbf{P}_{01} \mathbf{P}_{x1}^d \right. \\
& \cdot (\mathbf{I} - \mathbf{P}_{x1}^T)^{-1} \left( \sum_{i=0}^{T-1} \mathbf{P}_{x1}^i \right) \mathbf{P}_{x0} \left. \right] + (\mathbf{I} - \mathbf{P}_{10} \mathbf{P}^{k-1} - \mathbf{P}_{11} \mathbf{P}^{T-1})^{-1} \\
& \cdot \left[ \mathbf{P}_{00} + \mathbf{P}_{01} \left( \sum_{j=0}^{d-1} \mathbf{P}_{x1}^j \right) \mathbf{P}_{x0} + \mathbf{P}_{01} \mathbf{P}_{x1}^d (\mathbf{I} - \mathbf{P}_{x1}^T)^{-1} \mathbf{P}_{x1}^T (\mathbf{I} - \mathbf{P}_{x1}^T)^{-1} \right. \\
& \cdot \left. \left. \left( \sum_{i=0}^{T-1} \mathbf{P}_{x1}^i \right) \mathbf{P}_{x0} + 2\mathbf{P}_{01} \mathbf{P}_{x1}^d (\mathbf{I} - \mathbf{P}_{x1}^T)^{-1} \left( \sum_{i=0}^{T-1} \mathbf{P}_{x1}^i \right) \mathbf{P}_{x0} \right] \right\} \mathbf{1}
\end{aligned}$$

The throughput is the reciprocal of the expected transmission time ( $\eta = 1/\bar{\tau}$ ).

### 3.4 Delay Analysis

The matrix flow graph for delay analysis is shown in Figure 3.7. Nodes I, A, B and O represent the same states as in the throughput analysis. The transmitter receives a feedback at node A. There are four possibilities, an error-free ACK (transition to node O), an erroneous ACK (transition to node C), an error-free NACK (transition to node

B) and an erroneous NACK (transition to node G). Node G represents a NACK is lost and the transmitter is waiting for timeout and node C represents an ACK is lost and the frame will be acknowledged by a subsequent ACK/NACK. The self-loop around node C represent the delay from losing subsequent ACKs/NACKs. When the NACK is lost, the corresponding frame cannot be retransmitted immediately, but it will be retransmitted after timer expires, which involves a delay (transition from node G to node B). At node B, the lost frame will be retransmitted. Using basic manipulations, the matrix generating function of delay is

$$\begin{aligned}\Phi_D(z) &= z^{k-1} \mathbf{P}^{k-1} (\mathbf{I} - z^k \mathbf{P}_{10} \mathbf{P}^{k-1} - z^T \mathbf{P}_{11} \mathbf{P}^{T-1})^{-1} [z \mathbf{P}_{00} + z \mathbf{P}_{01} (\mathbf{I} - z \mathbf{P}_{x1})^{-1} z \mathbf{P}_{x0}] \\ &= \mathbf{P}^{k-1} (\mathbf{I} - z^k \mathbf{P}_{10} \mathbf{P}^{k-1} - z^T \mathbf{P}_{11} \mathbf{P}^{T-1})^{-1} [z^k \mathbf{P}_{00} + z^{k+1} \mathbf{P}_{01} (\mathbf{I} - z \mathbf{P}_{x1})^{-1} \mathbf{P}_{x0}]\end{aligned}$$

The generating function of delay can be computed as

$$\phi_D(z) = \frac{\pi_I \Phi_D(z) \mathbf{1}}{\pi_I \mathbf{1}}$$

where  $\pi_I$  can be also computed from the system of equations 3.3. Finally the average delay will be the derivative of  $\phi_D(z)$  at  $z = 1$ .

$$\begin{aligned}\bar{D} &= \left. \frac{d}{dz} \phi_D(z) \right|_{z=1} \\ &= \frac{1}{\pi_I \mathbf{1}} \pi_I \left\{ \mathbf{P}^{k-1} (\mathbf{I} - \mathbf{P}_{10} \mathbf{P}^{k-1} - \mathbf{P}_{11} \mathbf{P}^{t-1})^{-1} [k \mathbf{P}_{10} \mathbf{P}^{k-1} \right. \\ &\quad + t \mathbf{P}_{11} \mathbf{P}^{t-1}] (\mathbf{I} - \mathbf{P}_{10} \mathbf{P}^{k-1} - \mathbf{P}_{11} \mathbf{P}^{t-1})^{-1} [\mathbf{P}_{00} + \mathbf{P}_{01} (\mathbf{I} - \mathbf{P}_{x1})^{-1} \mathbf{P}_{x0}] \\ &\quad + \mathbf{P}^{k-1} (\mathbf{I} - \mathbf{P}_{10} \mathbf{P}^{k-1} - \mathbf{P}_{11} \mathbf{P}^{t-1})^{-1} [k \mathbf{P}_{00} + (k+1) \mathbf{P}_{01} (\mathbf{I} - \mathbf{P}_{x1})^{-1} \mathbf{P}_{x0} \\ &\quad \left. + \mathbf{P}_{01} (\mathbf{I} - \mathbf{P}_{x1})^{-1} \mathbf{P}_{x1} (\mathbf{I} - \mathbf{P}_{x1})^{-1} \mathbf{P}_{x0}] \right\} \mathbf{1}\end{aligned}$$

### 3.5 Numerical Results and Discussions

We consider channels with two states (good and bad). Let the state transition matrix be

$$\mathbf{P} = \begin{bmatrix} 1 - q & q \\ r & 1 - r \end{bmatrix}$$

where the first row and column corresponds to the good state ( $G$ ) and the second row and column to the bad state ( $B$ ). From the transition matrix, the stationary probability vector can be found using Equation 3.1. The probability of block error ( $\epsilon$ ) can be computed from the stationary vector and the probability of error in each state ( $\epsilon_G$  and  $\epsilon_B$ ). We will therefore use  $r, \epsilon, \epsilon_G$  and  $\epsilon_B$  as parameters of the forward channel. Note that  $1/r$  represents the average error burst. We assume that the reverse channel has the same parameters as the forward channel. As in GBN analysis, at least 1 million frames are simulated and the 95% confidence interval for all simulations lies within  $\pm 0.2\%$  of the reported results.

The two-state Markov channel is a special case of HMM where  $\epsilon_G$  and  $\epsilon_B$  equal 0 and 1 respectively. The throughput and delay of SR protocol in Markov channel is shown in Figure 3.8. As expected when the timer ( $T$ ) is increased, both throughput and delay are higher. The throughput is upper bounded by  $(1 - \epsilon)$  as  $T \rightarrow \infty$ ; naturally there is no such bound for delay.

The analytical and simulation results agree for the throughput. Simulation and analysis also agree for delay, except for a small difference in the case where the block error rates are high. The difference comes from the fact that a retransmitted frame might need to wait in retransmission queue. A frame will be retransmitted if its NACK is received or its timer expires. There is a possibility (especially when the block error rates are high) that a NACK is received for a frame and at the same time another frame's timer expires. In this case, one frame is retransmitted and the other frame has to wait in the queue.

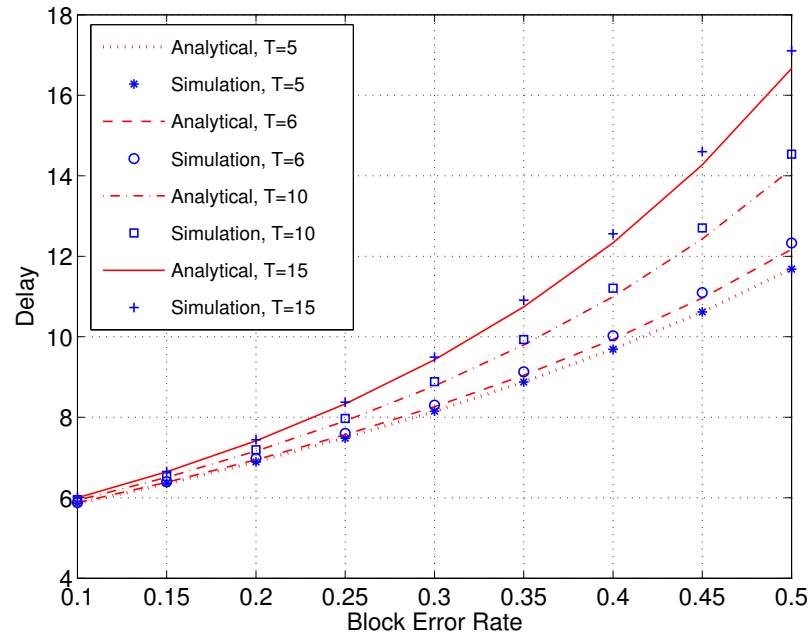
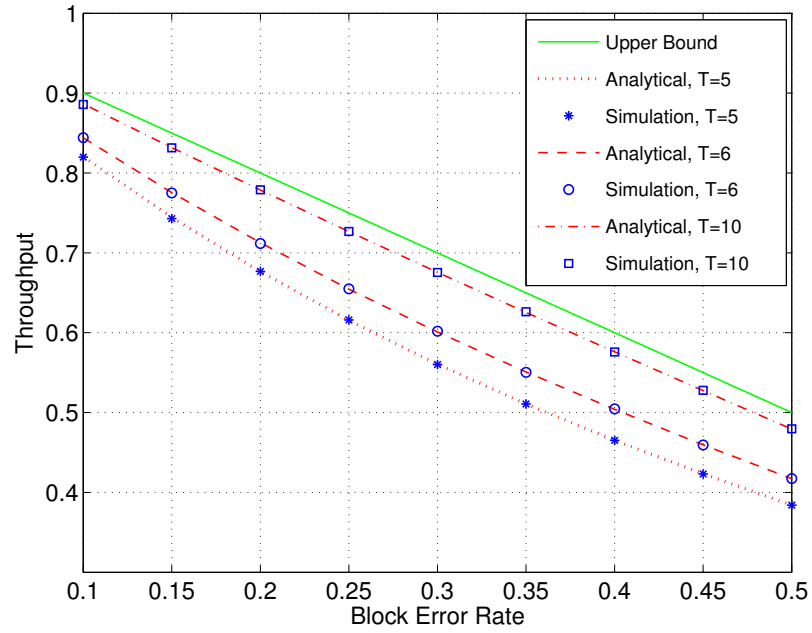


Figure 3.8. Throughput,  $\eta$  and delay,  $D$ , vs. block error rate,  $\epsilon$  in Markov errors for  $r = 0.3$  and  $k = 5$

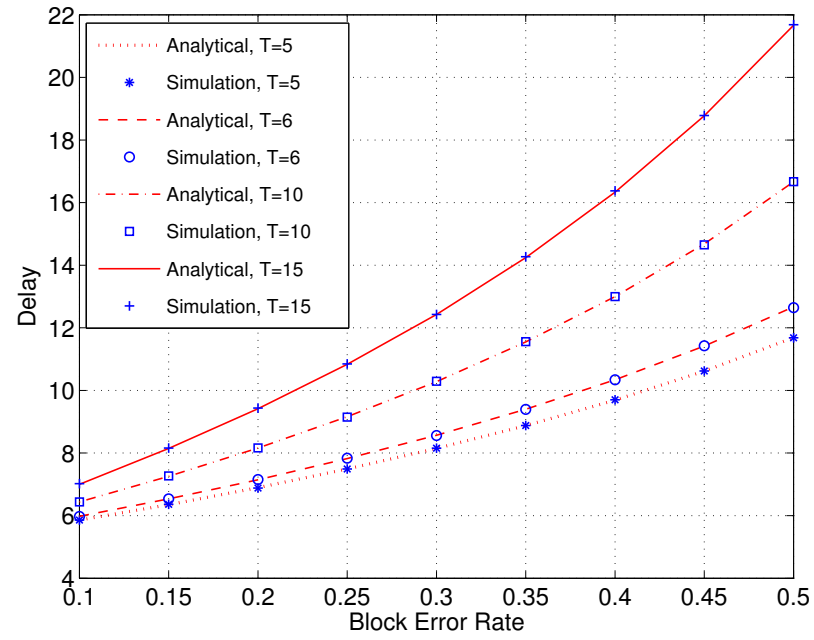
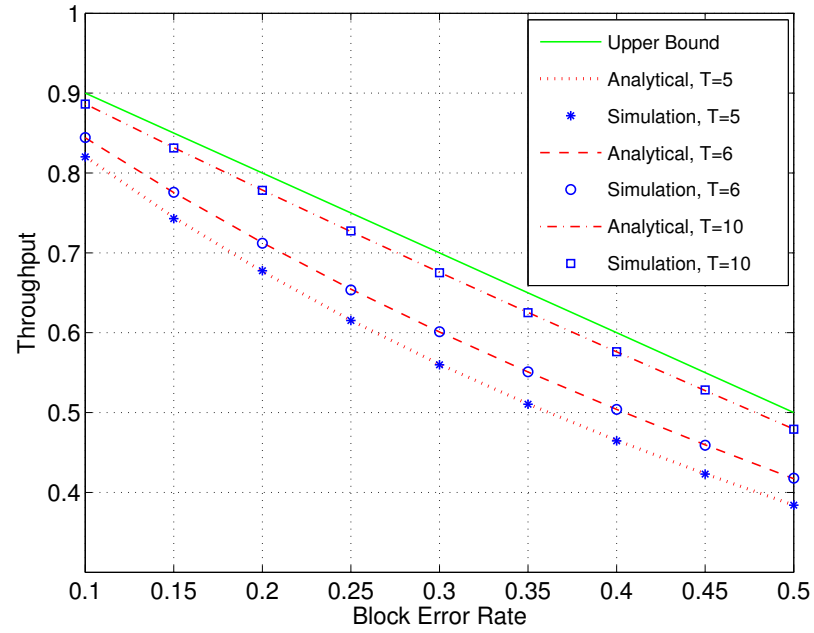


Figure 3.9. Throughput,  $\eta$  and delay,  $D$ , vs. block error rate,  $\epsilon$  in Markov errors without NACK for  $r = 0.3$  and  $k = 5$

To show that this is the only source of discrepancy, we analyze the SR protocol without NACK. When an erroneous frame is received, feedback is sent to update the transmitter about the receiver status. In this scenario, a frame is retransmitted only because of timer expiration so two frames cannot experience time-out at the same time (this is the source of the aforementioned discrepancy). We derive the expected throughput and delay in the same manner as before. Figure 3.9 shows that now, analytical and simulation results agree perfectly. Note the throughput of SR with and without NACK is almost the same. Similar behavior can also be observed from the SR performance in hidden Markov and block fading channels as shown in Figure 3.10, 3.11, 3.12 and 3.13.

We analyze the effect of timeout on the SR performance. The plots of the throughput and delay vs. timeout are shown in Figure 3.14. The plots compare the SR performance in both Markov and hidden Markov channels. With noiseless feedback, the error burst will not effect the SR throughput, a fact that has been reported in [10]. We see that the higher the error burst, the lower the SR throughput in noisy feedback. We also notice that the throughput in HMM is less sensitive to parameter  $r$ , compared to the Markov channel. Moreover the throughput approaches the bound faster in HMM than in Markov channel. Also note that the delay increases almost linearly with timeout. So the timeout should be configured such that the throughput is maximized, while maintaining acceptable delay.

Figure 3.15 compares two SR variations. In method  $SR_1$ , the feedback includes information about all successfully received frames while the information is excluded in method  $SR_2$ . For brevity, the we omit the flow graphs and analysis of the individual variations, and only mention that the same technique that was developed earlier in the paper was used for their analysis.

We observe that method  $SR_1$  has higher throughput and lower delay. Also, the throughput of  $SR_2$  is less sensitive to the value of timeout compared to  $SR_1$ , however,

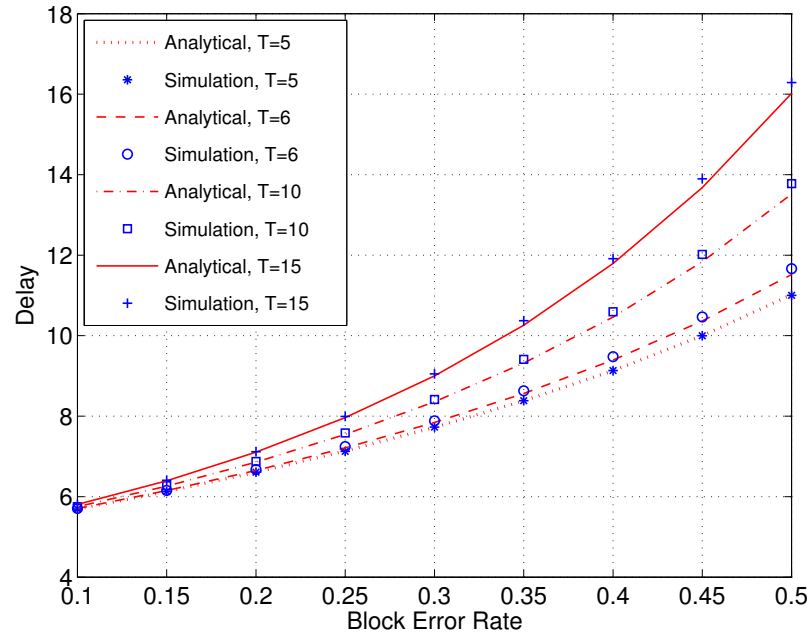
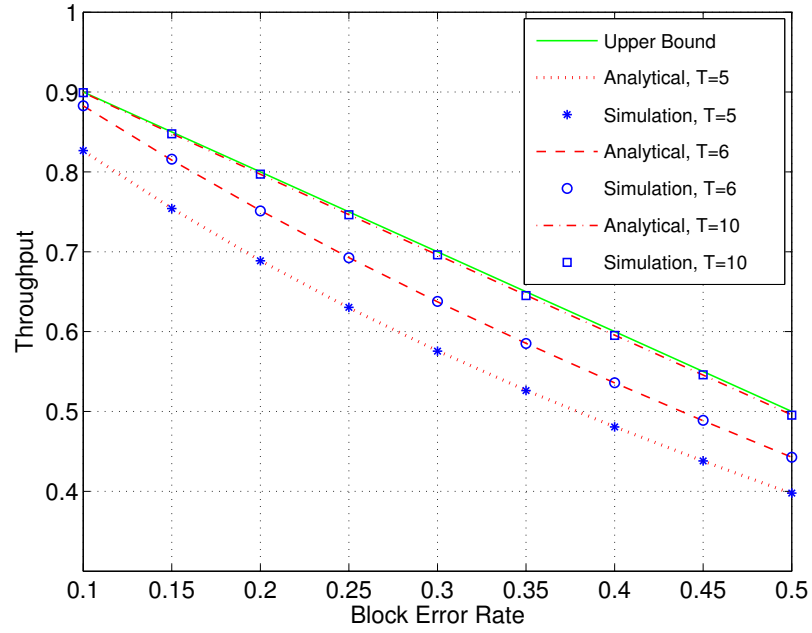


Figure 3.10. Throughput,  $\eta$  and delay,  $D$ , vs. block error rate,  $\epsilon$  in hidden Markov errors for  $r = 0.3$ ,  $\varepsilon_G = 0.07$ ,  $\varepsilon_B = 0.7$  and  $k = 5$

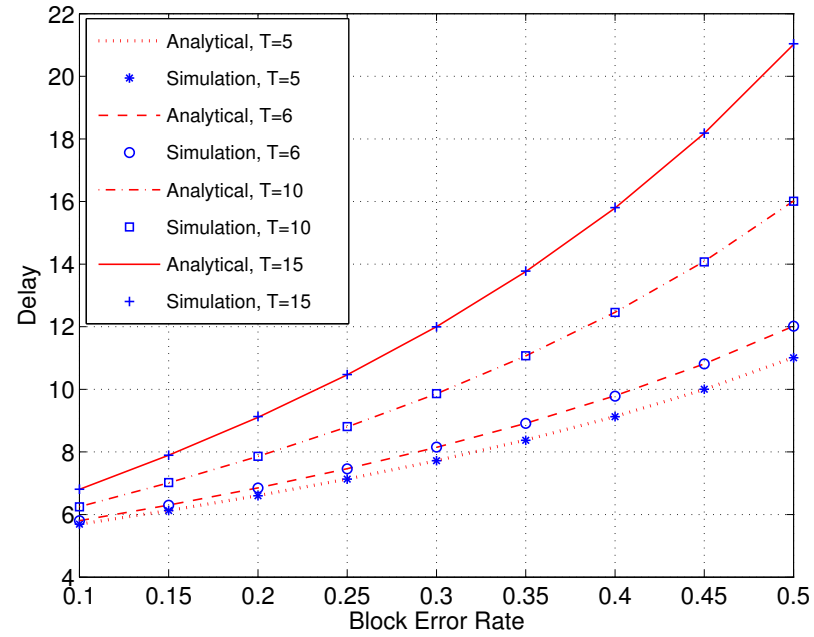
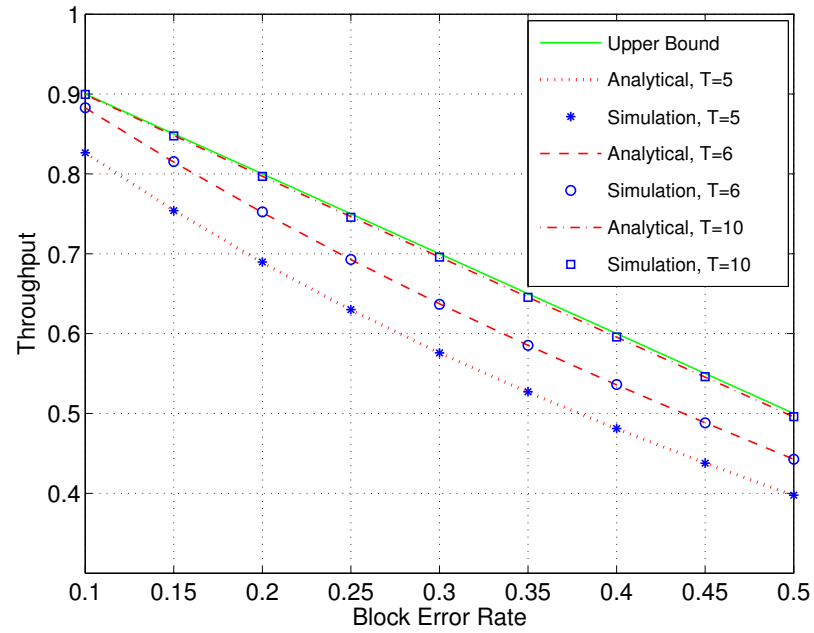


Figure 3.11. Throughput,  $\eta$  and delay,  $D$ , vs. block error rate,  $\epsilon$  in hidden Markov errors without NACK for  $r = 0.3$ ,  $\epsilon_G = 0.07$ ,  $\epsilon_B = 0.7$  and  $k = 5$

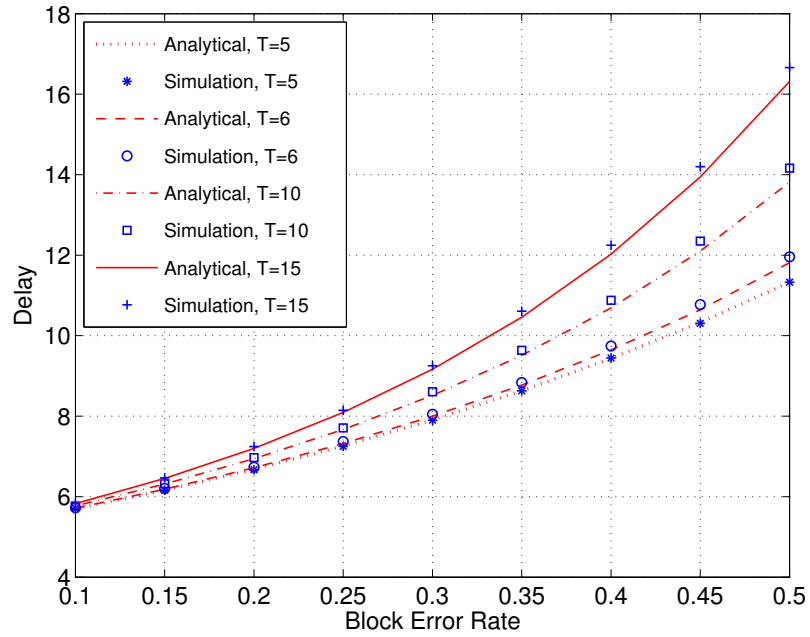
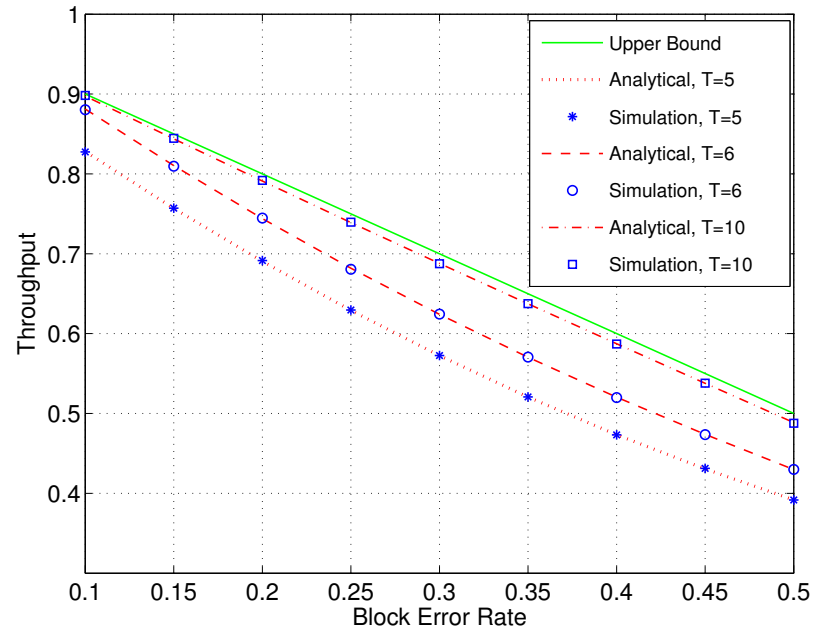


Figure 3.12. Throughput,  $\eta$  and delay,  $D$ , vs. block error rate,  $\epsilon$  in block fading for  $N = 3, r = 0.3, \varepsilon_G = 0.07, \varepsilon_B = 0.7$  and  $k = 5$

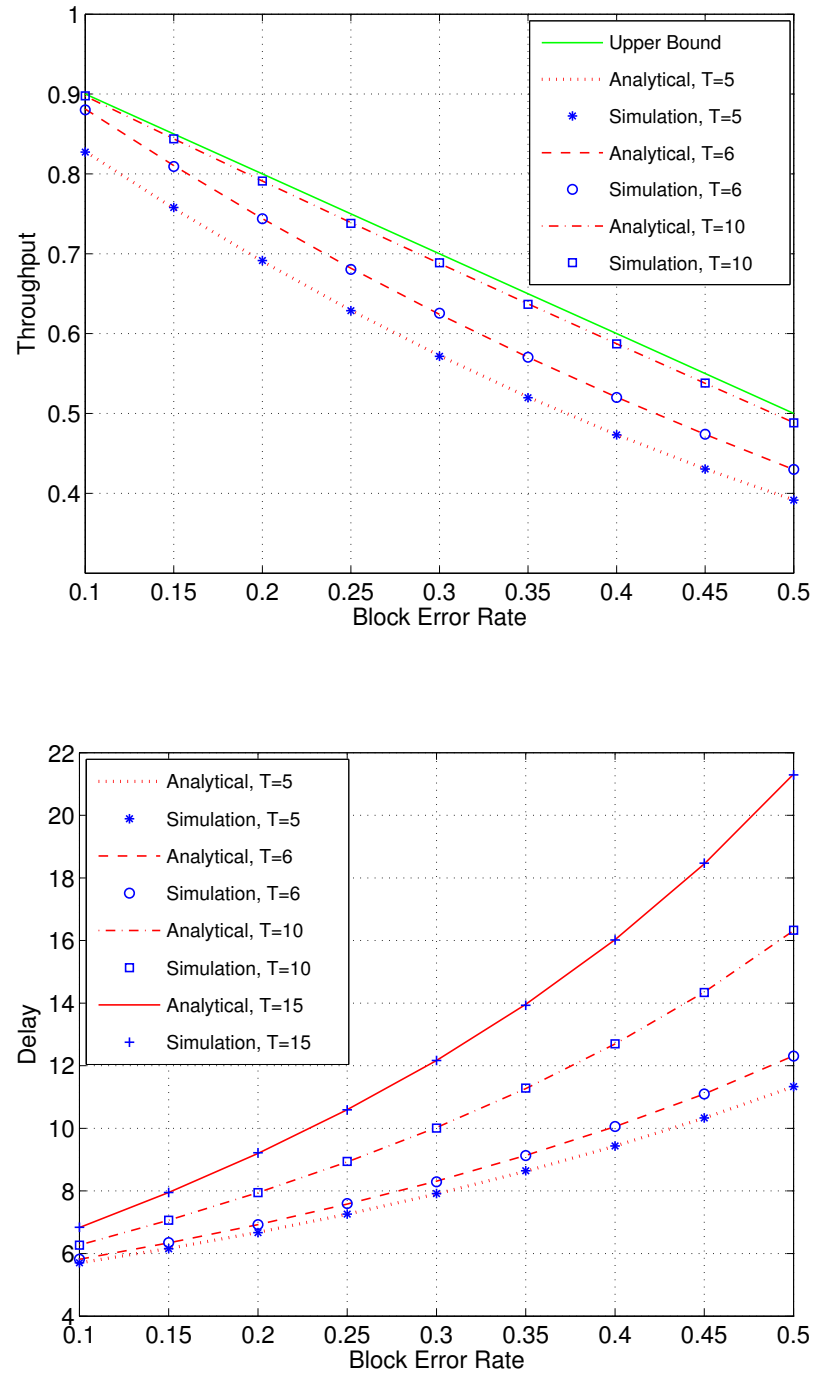


Figure 3.13. Throughput,  $\eta$  and delay,  $D$ , vs. block error rate,  $\epsilon$  in block fading with out NACK for  $N = 3, r = 0.3, \varepsilon_G = 0.07\varepsilon_B = 0.7$  and  $k = 5$

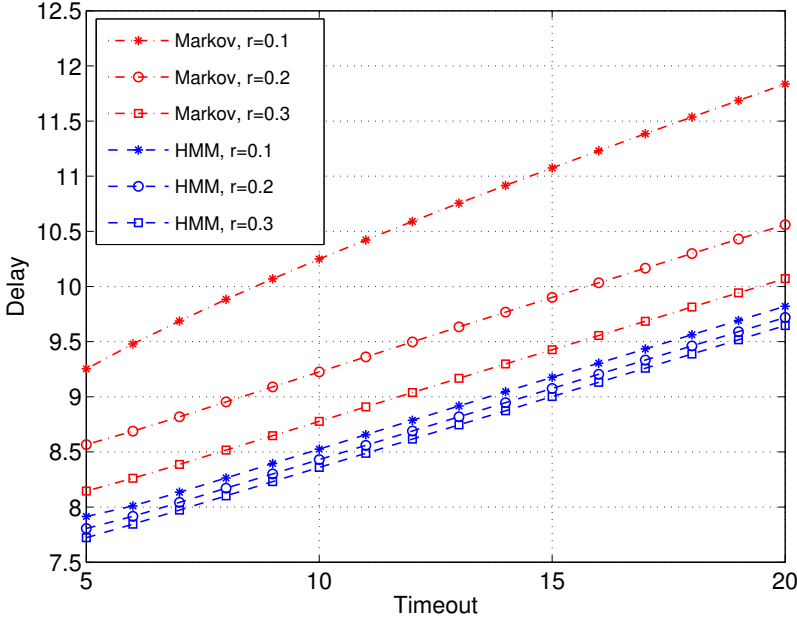
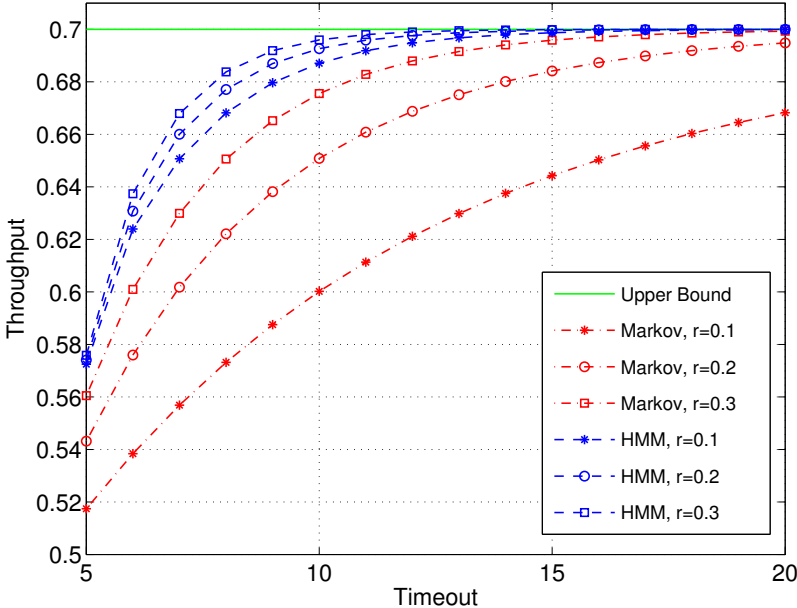


Figure 3.14. Throughput,  $\eta$  and delay,  $D$ , vs. timeout,  $T$  in Markov errors for  $\epsilon = 0.3$  and  $k = 5$  and in HMM for  $\epsilon = 0.3, \epsilon_G = 0.07, \epsilon_B = 0.7$  and  $k = 5$

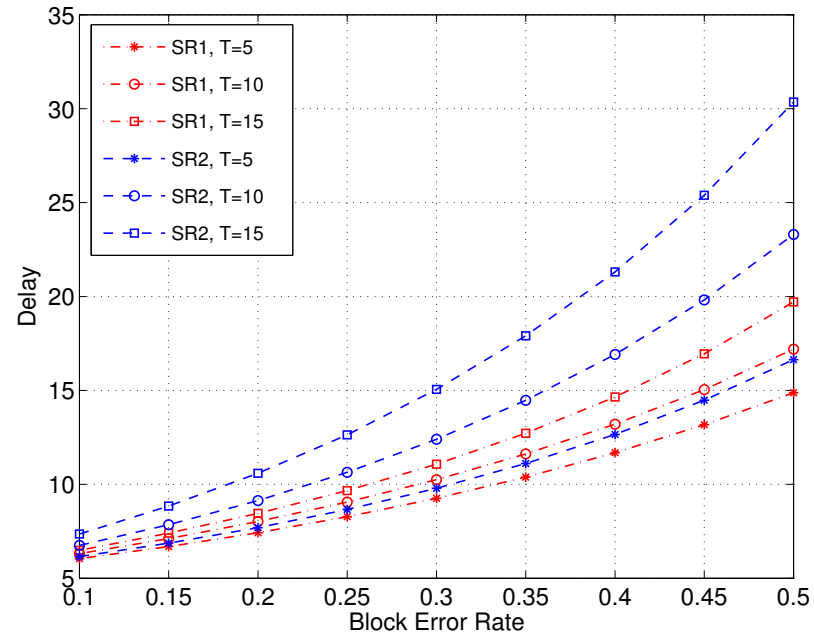
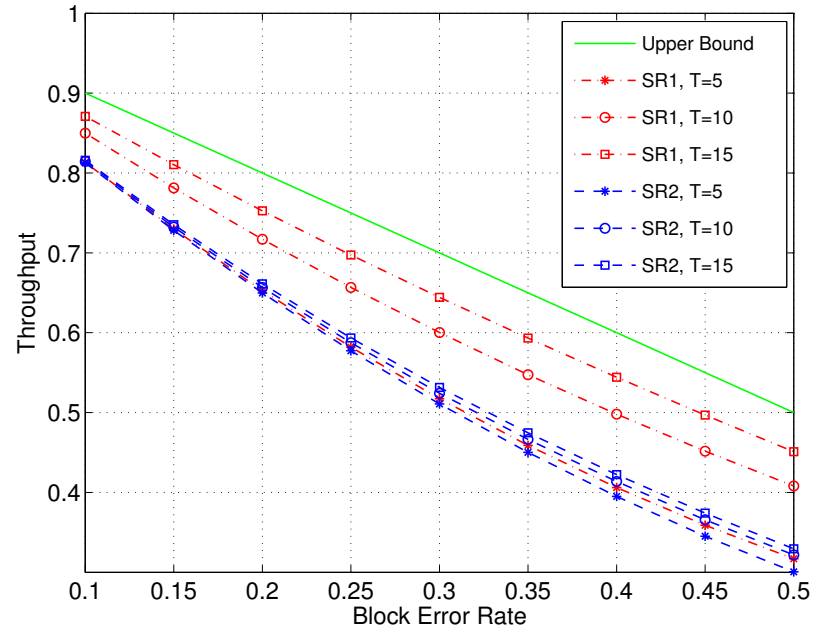


Figure 3.15. Throughput,  $\eta$  and delay,  $D$ , vs. block error rate,  $\epsilon$  in Markov errors for  $r = 0.1$  and  $k = 5$

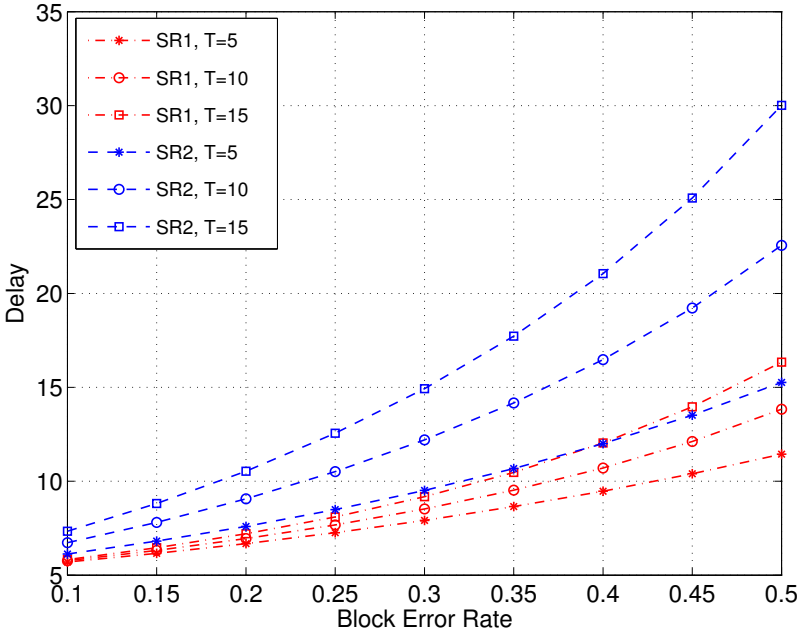
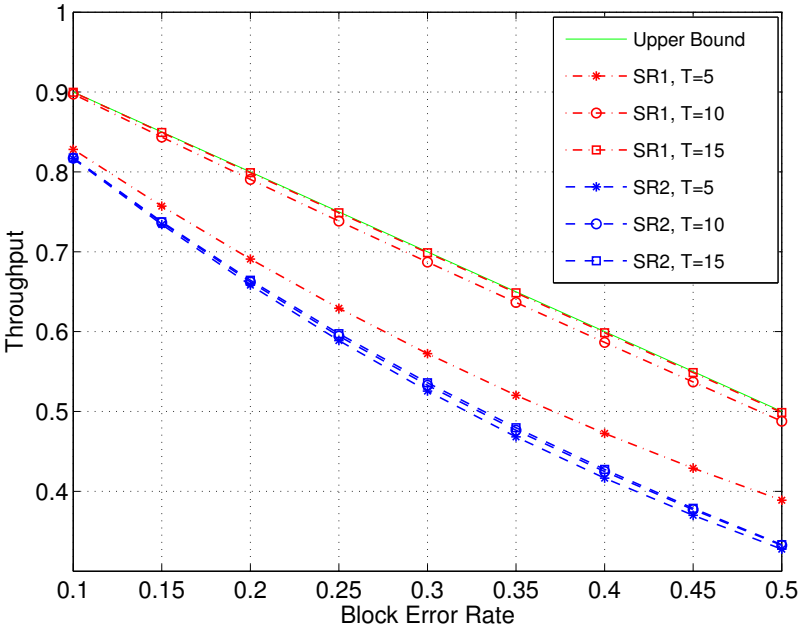


Figure 3.16. Throughput,  $\eta$  and delay,  $D$ , vs. block error rate,  $\epsilon$  in hidden Markov errors for  $r = 0.1$ ,  $\epsilon_G = 0.07$ ,  $\epsilon_B = 0.7$  and  $k = 5$

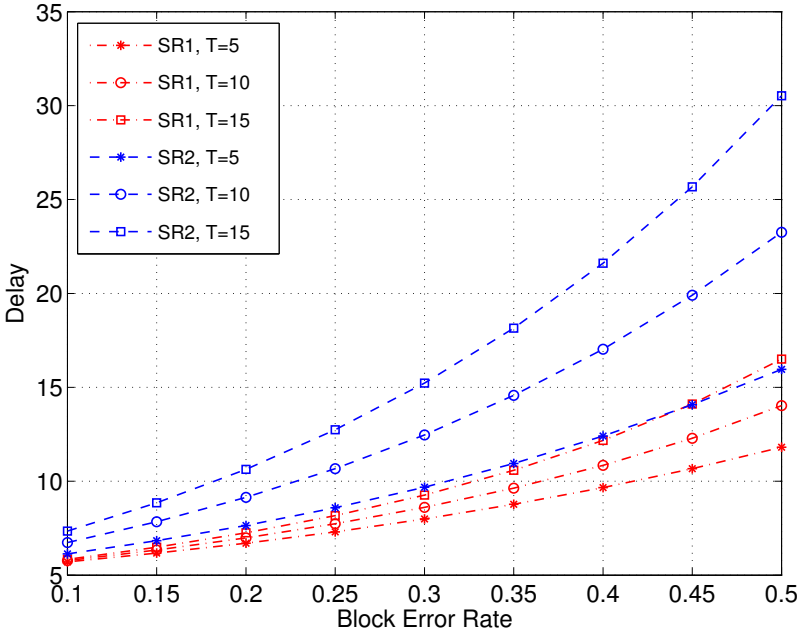
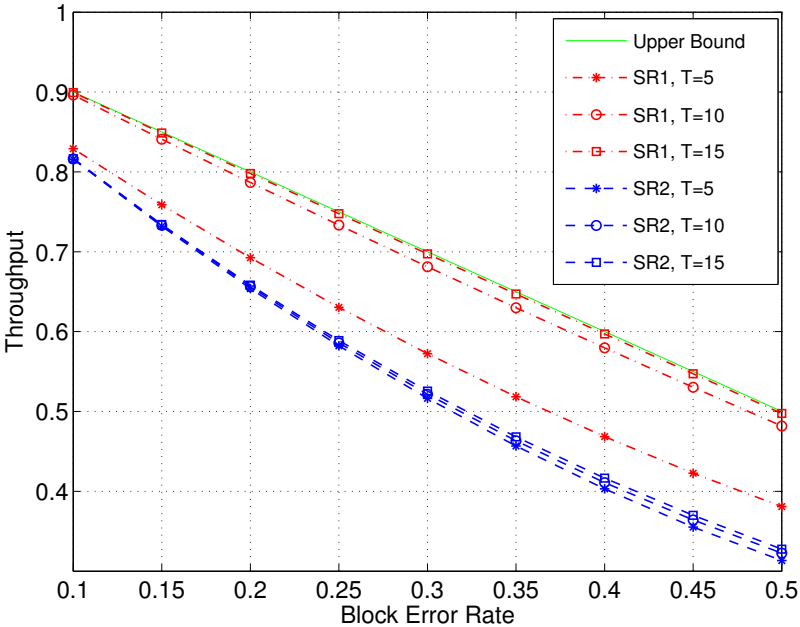


Figure 3.17. Throughput,  $\eta$  and delay,  $D$ , vs. block error rate,  $\epsilon$  in block fading for  $N = 3, r = 0.1, \epsilon_G = 0.07, \epsilon_B = 0.7$  and  $k = 5$

the delay of  $SR_2$  is more sensitive. Similar results are obtained in hidden Markov and block fading channels as shown in Figure 3.16 and 3.17 respectively.

### 3.6 Summary

We present a generalization of Mason's graphs to analyze the performance of Selective Repeat ARQ. We find the moment generating function (MGF) of transmission and delay time. Using the MGF, we calculate the average throughput and delay.

## CHAPTER 4

### CONCLUSION AND FUTURE WORK

We analyze the performance of two basic ARQ protocols, Go-Back-N (GBN) and Selective Repeat (SR). Our results can apply to any finite-state hidden Markov models on the forward and reverse channels. In SR analysis, we also present a new technique to derive the moment generating function.

We start in Chapter 2 by discussing a representation of a hidden Markov model (HMM) as described in [14]. Although this representation is not as streamlined as the canonical HMM representation, it simplifies calculations and plays an important role in our analysis. We show that block fading can also be characterized by a HMM. Using some of the results in [14], we calculate the throughput of GBN under block fading. We also calculate the throughput of GBN with erasure feedback errors and a timeout mechanism. These results are verified by simulations.

In Chapter 3, we calculate the throughput and delay of SR ARQ. We first present a generalization of Mason's graph with matrix weights, called matrix signal flow graphs (MSFG). Using MSFG, we derive the moment generating function (MGF) of transmission and delay time. Using the MGF, we calculate the throughput and delay of SR ARQ with erasure errors and a timeout mechanism. We analyze the effect of timeout on the throughput and delay, assuming that the feedback updates the transmitter about all correctly received frames. We also compare the performance of SR ARQ when the feedback either does or does not include information about previous frames.

Possible future directions include finding the delay time of GBN. Because GBN

only receives frames in order, the delay analysis has to take into account the transmission condition of previous frames. Moreover in GBN analysis, we focus mainly on the transmitter and ignore the receiver. GBN protocol with more advanced receivers has better performance and is frequently used in practice.

In SR analysis, we have analyzed the transmission delay. The delay analysis can be extended to include other delay time such as re-sequencing delay. Our analysis of SR ARQ ignores buffer overflow. In practice, it is unlikely that the receiver will have a infinite buffer. If there is a finite buffer, we expect the throughput of SR to be lower and the delay to be higher. An interesting problem is how the finite buffer will affect on the performance of SR so that we can get the expected throughput and/or delay with minimum buffer.

With matrix signal flow graphs, we can potentially analyze other protocols in hidden Markov channels. This extension can be very useful because a hidden Markov model can accurately describe wireless fading channels and the result will be in matrix form.

## BIBLIOGRAPHY

- [1] L. N. Kanal and A. R. K. Sastry, “Models for channels with memory and their applications to error control,” *Proc. of the IEEE*, vol. 66, pp. 724–744, Jul. 1978.
- [2] H. S. Wang and P.-C. Chang, “On verifying the first-order Markovian assumption for a Rayleigh fading channel model,” *IEEE Trans. Veh. Technol.*, vol. 45, no. 2, pp. 353–357, May 1996.
- [3] M. Zorzi, R. R. Roa, and L. B. Milstein, “On the accuracy of a first-order Markov model for data transmission on fading channels,” in *Proc. IEEE ICUPC*, Nov. 1995, pp. 211–215.
- [4] H. S. Wang and N. Moayeri, “Finite-state Markov channel—A useful model for radio communication channels,” *IEEE Trans. Veh. Technol.*, vol. 44, no. 1, pp. 163–171, Feb. 1995.
- [5] Q. Zhang and S. A. Kassam, “Finite-state Markov model for Rayleigh fading channels,” *IEEE Trans. Commun.*, vol. 47, no. 11, pp. 1688–1692, Nov. 1999.
- [6] C. C. Tan and N. C. Beaulieu, “On first-order Markov modeling for the Rayleigh fading channel,” *IEEE Trans. Commun.*, vol. 48, no. 12, pp. 2032–2040, Dec. 2000.
- [7] P. Bergamo, D. Maniezzo, A. Giovanardi, G. Mazzini, and M. Zorzi, “An improved Markov chain description for fading processes,” in *Proc. IEEE ICC’02*, Apr.-May 2002, pp. 1347–1351.
- [8] W. Turin and R. van Nobelen, “Hidden Markov modeling of flat fading channels,” *IEEE J. Select. Areas Commun.*, vol. 16, no. 9, pp. 1809–1817, Dec. 1998.

- [9] C. H. C. Leung, Y. Kikumoto, and S. A. Sorensen, "The throughput efficiency of the Go-Back-N ARQ scheme under Markov and related error structures," *IEEE Trans. Commun.*, vol. 36, pp. 231–234, Feb. 1988.
- [10] D. L. Lu and J. F. Chang, "Performance of ARQ protocols in nonindependent channel errors," *IEEE Trans. Commun.*, vol. 41, no. 5, pp. 721–730, May 1993.
- [11] S. R. Kim and C. K. Un, "Throughput analysis for two ARQ schemes using combined transition matrix," *IEEE Trans. Commun.*, vol. 40, no. 11, pp. 1679–1683, Nov. 1992.
- [12] Y. J. Cho and C. K. Un, "Performance analysis of ARQ error controls under Markovian block error pattern," *IEEE Trans. Commun.*, vol. 42, pp. 2051–2061, Feb.-Apr. 1994.
- [13] M. Zorzi and R. R. Rao, "Throughput analysis of Go-Back-N ARQ in Markov channels with unreliable feedback," in *Proc. IEEE ICC'95*, Jun. 1995, pp. 1232–1237.
- [14] W. Turin, "Throughput analysis of the Go-Back-N protocol in fading radio channels," *IEEE J. Select. Areas Commun.*, vol. 17, no. 5, pp. 881–887, May 1999.
- [15] M. Zorzi and R. R. Rao, "Throughput performance of ARQ selective-repeat protocol with time diversity in Markov channels," in *Proc. IEEE GLOBECOM*, Nov. 1995, vol. 3, pp. 1673–1677.
- [16] M. Zorzi and R. R. Rao, "Bounds on the throughput performance of ARQ selective-repeat protocol in Markov channels," in *Proc. IEEE GLOBECOM*, Jun. 1996, vol. 2, pp. 782–786.

- [17] J. G. Kim and M. M. Krunz, “Delay analysis of selective repeat ARQ for a Markovian source over a wireless channel,” *IEEE Trans. Veh. Technol.*, vol. 49, no. 5, pp. 1968–1981, Sep. 2000.
- [18] M. Rossi, L. Badia, and M. Zorzi, “Exact statistic pf ARQ packet delivery delay over Markov channels with finite round-trip delay,” in *Proc. IEEE GLOBECOM*, Dec. 2003, vol. 6, pp. 3356–3360.
- [19] M. Rossi, L. Badia, and M. Zorzi, “SR-ARQ delay statistics on N-state Markov channels with finite round trip delay,” in *Proc. IEEE GLOBECOM*, Nov.-Dec. 2004, vol. 5, pp. 3032–3036.
- [20] W. Luo, K. Balachandran, S. Nanda, and K. K. Chang, “Delay analysis of selective-repeat ARQ with applications to link adaptation in wireless packet data systems,” *IEEE Trans. Wireless Commun.*, vol. 4, no. 3, pp. 1017–1029, May 2005.
- [21] R. J. McEliece and W. E. Stark, “Channels with block interference,” *IEEE Trans. Inform. Theory*, vol. IT-30, no. 1, pp. 44–53, Jan. 1984.
- [22] D. L. Lu and J. F. Chang, “Analysis of ARQ protocols via signal flow graphs,” *IEEE Trans. Commun.*, vol. 37, no. 3, pp. 245–251, Mar. 1989.
- [23] S. J. Mason, “About such things as unistors, flow graphs, probability, partial factoring and matrices,” *IRE Trans. Circuit Theory*, vol. CT-4, pp. 90–97, Sep. 1957.
- [24] W. Turin, *Performance Analysis and Modeling of Digital Transmission Systems*, Kluwer Academic/Plenum Publishers, New York, New York, 2004.
- [25] R. A. Howard, *Dynamic Probabilistic Systems*, John Wiley & Sons, Inc., New York, 1971.

- [26] S. J. Mason and H. J. Zimmermann, *Electronic, Circuits, Signals, and Systems*, John Wiley & Sons, Inc., New York, 1960.

## VITA

Kamtorn Ausavapattanakun was born in Bangkok, Thailand, on November 9, 1975, the eldest son of Kittti and Tarinee Asvapathanagul. He graduated in 1992 from the Suankularb Wittayalai High School, Bangkok, Thailand. He received the Bachelor of Engineering degree in Electronics and Telecommunications from King Mongkut's Institute of Technology, Thonburi, Thailand in March 1996. Since January 2003, he has been studying towards a Master of Science degree at the University of Texas at Dallas, Richardson, USA.

Permanent address: 555/13, Soi 17, Pracharat 1 Rd., Bangsue,  
Bangkok 10800 THAILAND

This thesis was typeset with L<sup>A</sup>T<sub>E</sub>X<sup>†</sup> by the author.

---

<sup>†</sup>L<sup>A</sup>T<sub>E</sub>X is a document preparation system developed by Leslie Lamport as a special version of Donald Knuth's T<sub>E</sub>X Program.